BENEFITS OF PHASED ARRAY ANTENNA CONFIGURATIONS IN HEXAGONAL CELLS

A Thesis

by

ALEXANDRU RADUCANU

Submitted to the Office of Graduate and Professional Studies of
Texas A&M University
in partial fulfillment of the requirements for the degree of

MASTER OF SCIENCE

Chair of Committee,	Jean-Francois Chamberland
Co-Chair of Committee,	Gregory H. Huff
Committee Members,	Krishna R. Narayanan
	Joseph H. Ross Jr.
Head of Department,	Miroslav M. Begovic

August 2015

Major Subject: Electrical Engineering

ABSTRACT

In this research a series of studies are conducted, which focus on obtaining an optimal signal strength based on an evaluation of downlink and uplink performance. Furthermore, the goal of this research is to determine a phased array antenna configuration which performs best given a specific environment. To accomplish this, three phased array antenna configurations (1 by 16, 2 by 8, and 1 by 16) are proposed in an environment containing distributed interferers. The environment consists of a hexagonal cellular structure, which is a geometrical implementation currently utilized by cell phone towers in the telephony systems. Interferers are placed at given locations throughout the cell to represent other users which could disturb the reception from intended receivers. With the results obtained, several conclusions were drawn about the performance of each antenna. First, if the transfer of information is of uttermost importance, and no regard is given toward signal integrity, interference, or jamming, the 4 by 4 PAA configuration would be the best candidate. Second, if interference is rampant and a high priority is given toward signal integrity, the 1 by 16 or 2 by 8 PAA configuration would be the best performers. Lastly, the 1 by 16 shows the lowest average interference; however, in comparison to the 2 by 8, the 1 by 16 PAA has a larger variance in the spread of this interference.

ACKNOWLEDGMENTS

I would like to thank my advisor, Dr. Jean-François Chamberland, not only for his constant guidance and support but also for making this experience one of the most enjoyable and rewarding opportunities I have been a part of in college.

NOMENCLATURE

PAAs	Phased Array Antennas
EMWs	Electromagnetic Waves
AP	Access Point
SINR	Signal to Interference plus Noise Ratio
FCC	Federal Communications Commission
ISM	Industrial Scientific Medical

TABLE OF CONTENTS

Page

LIST OF FIGURES

FIGURE Page

LIST OF TABLES

CHAPTER I

INTRODUCTION

Breakdown of Chapters

This section summarizes this study by detailing the main focus of each chapter and providing a descriptive outline which the reader can follow.

Chapter I: Introduction

The main purpose of this chapter is to introduce the reader to phased array antennas and the research conducted in this study. The chapter begins by providing a short description of what a phased array antenna system is and how it establishes communication. Next, the benefits, difficulties, and design constraints encountered in establishing communication with a user are covered, in order to show the motivation behind this study. To familiarize the reader with the path antenna research has traversed, a brief history and continuation of previous research is addressed after. At the end of this chapter, the Wi-Fi protocol used in this study is introduced and elaborated on.

Chapter II: Background

This chapter focuses on presenting the necessary knowledge needed to understand how a phased array antenna system works in uplink and downlink scenarios. The basics are covered first, after which more detail is given on radiation fields. Next, the construction of linear phased arrays and planar phased arrays as well as the equations needed to

represent radiation patterns created by these arrays follow. The limitations and restrictions imposed on phased arrays are further emphasized in this chapter: side lobes, grating lobe positions, and the beamwidth of the radiation pattern. In the last four sections of Chapter II, the quantification of downlink and uplink performance is cover. The free space path loss is described and equations related to downlink and uplink conclude the chapter.

Chapter III: System Model

The purpose of this chapter is to present all the variables which were considered and determined in this study. The chapter begins by first depicting the area in which the antenna is to be utilized, then detailing the dimensions of the antenna towers. Within this area the receivers and interferers density and locations are then established. After these setting parameters are determined, the phased array antenna properties are concluded within each section. These properties are: the antenna phased array elements' dimensions, the number of elements, the arrangement of elements (geometry and element distance), the wavelength of transmission and reception, and lastly the configuration of these elements (1 by 16, 2 by 8, and 4 by 4). The next sections cover the creation of the radiation patterns, after which the mapping of the patterns on the area is described. The chapter ends with the revisiting of the downlink and uplink procedures.

Chapter IV: Simulated Results

This chapter focuses on the obtained simulated results from the system model determined in Chapter III and the theoretical background established in Chapter II. First, the operational area is revisited to show the placement of receivers and transmitters. After which, the quantitative results are showed numerically and graphically. The radiation patterns, projections on the area, and applied path loss and interpolation of each antenna configuration (1 x 16, 2 x 8, and 4 x 4) is depicted. The chapter concludes with the efficiency results obtained for both the uplink and downlink communication procedures.

Chapter V: Conclusion

This chapter finalizes the study and summarizes the results obtained.

Preliminaries

Phased array antennas (PAAs) consist of multiple stationary antenna elements that are fed coherently and use variable phase or time delay control at each element to scan a beam to some given angle in space. The two main reasons PAA are used are: 1) to create a more directional beam from multiple antenna elements and 2) to redirect this beam electronically rather than mechanically in space [1]. The beam created is a radiation pattern consisting of electromagnetic waves (EMWs) with a particular frequency, which depends on the antenna properties. The EMWs carry information based on a protocol that is set at an access point (AP). To successfully transmit the information encoded, the

EMWs must reach a user with sufficient power and exceed a prescribed noise threshold. If the signal reaches the user successfully, it can be decoded assuming the user knows the protocol used to encode the signal.

Motivation

Phased array antennas are greatly increasing in popularity. They are no longer a sole object of military (radar) systems, but today are encountered in many civilian systems, such as mobile communications and wireless base stations [6]. Furthermore, phased arrays are continuing to replace traditional directional antennas due to the benefits they provide from their electronic configurability.

Within this communication process, numerous difficulties arise in the transmission and reception of the signal. First, the configuration of the PAA will impact the accuracy, directivity, and strength with which the signal is transmitted. Second, the individual antenna elements will impact the directivity, and transmission frequency. Third, the phase shifting resolution will impact the angular directivity of the beam. Fourth, the amount of power used will impact the radius of transmission. Lastly, the spatial settings such as geographical landscape or density and proximity of interferes will impact the reliability of the signal. These issues are addressed in this work, in order to determine an antenna array configuration which is most effective in a given scenario.

The current increase of technological advancements in wireless communication has also increased the demand for faster and more dependable transfer of information. With these demands, great research emphasis has been placed on addressing these needs. One method of significant interest has been the deployment of "cellular base station phased array antenna systems" because phased arrays are capable of solving several issues which pertain to user-to-base-station uplink and downlink [3]. Some of the benefits phased arrays can provide are: 1) increase the overall gain of the antenna, 2) provide diversity of reception, 3) cancel interference from a particular set of directions, 4) steer the array beam in a specific direction, 5) determine the direction of arrival of incoming signals, and 6) maximize the signal to interference plus noise ratio (SINR) [4]. Due to these benefits, antenna arrays are being integrated in Wi-Fi routers or wireless LAN access points as well.

Although phased array antennas provide significant advantages, they also add constraints which increase the difficulty in developing accuracy and efficiency. Several design parameters are important in the development of an active PAA which is portable: size, reliability and accuracy, power, and cost. The first parameter which dictates the portability of the phased array is size. The antenna needs to have a relatively small aperture; however by decreasing the aperture or surface area of the antenna a decrease in the reliability and accuracy of transmission will be experienced. The second parameters to consider are the reliability and accuracy of transmission within an area. The antenna must achieve a certain degree of accuracy in directing its main beam toward intended

receivers, especially in scenarios in which interference or jamming from other users in the area is experienced. A narrow beam is required to locate receivers with accuracy. Furthermore, the antenna must be reliable in transmitting a signal with sufficient power to reach the receiver. The third parameter which also dictates the efficiency of the antenna is power consumption or power output. One strict regulation on the antenna is that the unit needs to meet power constraints which are set by the Federal Communications Commission (FCC). To satisfy a portable system, limited power is available for the transmission of wireless signals. In turn, a low power realization requires the antenna system to have high gains implemented in order to transmit across larger distances. The final and most rigorous design requirement is low cost. Although the antenna system may satisfy the previous three constraints, it will not be marketable with a high price tag. The largest percentage of the cost within this system lies in the manufacturing of each antenna element and its associated transmission and reception hardware. Therefore cost per antenna element implemented is a critical design parameter [4]. These four design constraints: size, reliability and accuracy, power, and cost, are the primary factors that govern the use of antenna arrays in large scale commercial applications.

Wireless Protocol (Wi-Fi 802.11)

To develop a successful means of communication the first step is to define a frequency and protocol with which both receiver and transmitter will operate. There are many ways of communicating wirelessly. The protocol which was chosen for this project is the

802.11 Wi-Fi protocol because it caters to most of the PAAs design constraints previously mentioned.

The Wi-Fi standard operates on 12 channels from the 2.4 GHz to 2.5GHz in the microwave frequency band and is the most widely implemented wireless communication protocol [5]. It is regulated by the Federal Communications Commission (FCC) in the United States. The FCC has designated the 2.4 GHz to 2.5 GHz, industrial scientific medical (ISM) frequency band, as a license free band for radio communications. Thus, in this radio spectrum there are no license requirements or fees in transmitting or receiving within this frequency band. The equipment that transmits at these frequencies however must be regulated by the FCC. In accordance to the FCC: "equipment which is utilized to transmit within the WLAN frequency must adhere to design radio frequency, output power levels, and indoor/outdoor environment requirements and limitations" [5].

With regards to the FCC regulations, it is fairly easy to deploy an antenna system capable of transmitting within the Wi-Fi frequency because the Wi-Fi Alliance ensures that certified products are standardized to function within this wireless spectrum [5]. Another great benefit is that Wi-Fi has a very small physical footprint when compared to the wireless spectrum as shown in Fig. 1. [5]. For this reason, the deployment of Wi-Fi antennas can be conducted with very low cost. The Wi-Fi antenna can be strategically deployed to communicate with users within a certain area. These users do not need to form a line of sight with the antenna; as long as they are within the maximum range of

transmission, the wireless antenna or access point can form a link which can sustain communication. This can be accomplished with equipment of relatively low cost on the receiver end. Another great benefit of the Wi-Fi protocol is its mobility and flexibility [5].With the deployment of a Wi-Fi equipped AP, transmitting information in a remote location can be easily accomplished. Lastly, Wi-Fi technology is embedded in many smart phones and tablets of present day. Receivers of many shapes and sizes currently exist and can readily be used in communicating with Wi-Fi beacons; these receivers do not need to be built or reconfigured. These benefits of the Wi-Fi protocol meet some of the previously mentioned design constraints of a portable PAA system, and for this reason it was chosen as the communication protocol to be used in this project.

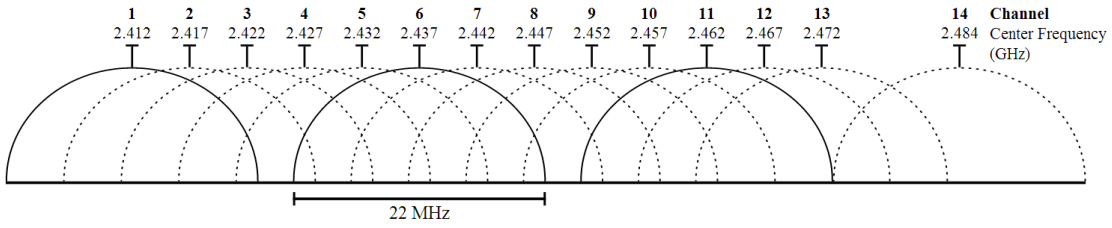

Fig. 1. A graphical representation of the Wi-Fi spectrum with the labeling of each channel. There are 14 channels from 2.412 GHz to 2.484 GHz with a bandwidth of 22 MHz, leaving 3 non overlapping channels [20].

History

A brief history is covered in this section to illustrate the immense path antenna research has traversed throughout time and to familiarize the reader with the accomplishments

which led up to the current research. Refer to [6] for a more detailed account of these events.

Maxwell

The era of wireless communications began in the 1860s when James Clerk Maxwell, a Scottish Physicist, predicted the existence of radio waves.

Hertz

However, it was not until 20 years later, in 1886 that antennas were successfully introduced as a means of communication by Heinrich Hertz. Hertz created the antenna to experimentally verify Maxwell's theory and reported his results in a paper titled "The Forces of Electric Oscillations Created According to Maxwell's Theory". Hertz's experiment consisted of a transmitting dipole antenna and a receiving coil (loop antenna). He subsequently improved on his design by employing two parabolic reflector antennas, which he used to conduct radio beaming experiments over distances of up to 16 meters. After Hertz's death, his work was put into practice commercially by Guglielmo Marconi.

Marconi

Marconi started out his experiments like Hertz, using cylindrical parabolic reflectors fed in the focal point by half wave dipole antennas at a frequency of 1.2 GHz. With his equipment working at these microwave frequencies he could transmit messages over a

distance of several meters. In 1895, Marconi made some important changes to his system that allowed him to transmit and receive messages over distances of up to 1.5 km. He elevated one of the plates of his antenna in the air and connected the other to the ground. With this setup Marconi enlarged the antenna area and formed a half wave dipole. This created a wavelength larger than any that had been studied before.

Marconi had discovered that by increasing the aperture of the antenna he was able to adapt his radio system for longer wavelengths (lower frequencies) and made wireless communication possible over increased distances. This creation of long wavelength EMWs was the key to his success. Although he implemented this discovery successfully, he did not derive his success from putting theory into practice. It was not until later that the relation between antenna length and the operational wavelength of a radio system was explained by his colleague Prof. Roscoe Lee Webb, who calculated that the length of the wave radiated was four times the length of the vertical conductor.

In the next few years, Marconi's most technical challenge was establishing transatlantic wireless telegraph communication. Marconi pursued these experiments and on December 12, 1901 the Morse code for the letter "S" was sent from Cornwall Great Britain and received in Newfoundland Canada traveling a distance of 3684 km. In 1907, a reliable transatlantic telegraph was implemented and Marconi received the Nobel Prize in physics for these accomplishments along with Karl Ferdinand Braun in 1909.

Braun

In 1905, the phased array antenna was invented by Karl Ferdinand Braun. Braun received the Nobel Prize for his accomplishments and implementation of a three element antenna, which he published in his Nobel Lecture: *Electrical oscillations and wireless telegraphy* [7].

World War I

In 1914, the First World War started. At the outbreak of the war, telegraphy and telephony were still in their infancy; however, at sea the British Navy already had experience in using wireless communication. Many advancements in wireless communication emerged during this time as Marconi volunteered for the Italian Army and was appointed as lieutenant in charge of air ship engineering. During this time, Marconi built the first apparatus for wireless communications from aircraft to ground station for the Italian Army. Throughout the wars direction finding, message interception, crypto analysis, and jamming techniques gained tremendous interest and rapidly developed.

Between the Wars

In 1910, Lee de Forest developed a transmitter capable of broadcasting music. However, Forest had not realized the capability of his device to be used for voice transmission and in 1913 sold the rights to American Telephone and Telegraph Company (AT&T). In 1920, broadcasts started on a regular basis and, in 1922, the British Broadcasting

Corporation (BBC) was formed. The following year, in 1923, AT&T Corporation succeeded in accomplishing the first transatlantic wireless telephony connection between, Rock Key Point, New Jersey, and Southgate, England [6].

Cellular Era

In the years following the Second World War, much growth occurred in the development of radio frequency circuit design due to the growth of cellular technology. This growth brought about technological generations which featured different implementation standards, capacities, and mobile techniques with the goal of improving on the previous generation's performances. Several factors influenced the pursuit of cellular technologies. Some of the benefits sought were: "1) spectrum efficiency of operating in minimal bandwidth, 2) Relative to 'wired', wireless networks are, in most cases, cheaper to install and maintain, 3) Capacity system for mobile telephone will be high because a large number of subscribers cannot create blocking probability due to large coverage area" [8]. With the improvement of technology through time, the telephony generations continued to increase consecutively from 0G, 1G, 2G, 3G, 4G and presently to 5G.

Continuation

This research is a continuation of *A Cognitive Phased Array Using Smart Phone Control*, a previous phased array construction, by Jeffrey Scott Jensen in the Wireless and Communication Laboratory at Texas A&M University [22]. In this research a series

of studies were conducted, which focus on obtaining an optimal signal strength based on an evaluation of downlink and uplink performance. Furthermore, the goal of this research was to determine a phased array antenna configuration which performs best given a specific environment. To accomplish this, three phased array antenna configurations (physical and geometric designs) were proposed in an environment containing distributed interferers. The environment consists of a hexagonal cellular structure, which is a geometrical implementation currently utilized by cell phone towers in the telephony systems. Interferers are placed at given locations throughout the cell to represent other users which could disturb the reception from intended receivers.

CHAPTER II

BACKGROUND

Basics of Antennas

An antenna is a piece of hardware that is used to transmit or receive a radiating electromagnetic wave. The antenna changes electrical currents into electromagnetic waves and vice versa [9]. For antennas to function, they are usually connected to a transmitter or receiver. When the antenna is transmitting, a transmitter supplies an electric current oscillating at a certain frequency to the antenna terminals; the antenna radiates the energy from this current as electromagnetic waves [9]. When the antenna is receiving, it captures some of the power of an electromagnetic wave and produces a tiny voltage at its terminals; this voltage is applied to a receiver to be amplified and further analyzed [9]. In order to depict certain characteristics of the electromagnetic waves created by an antenna, a radiation pattern is utilized. A radiation pattern is a graphical representation of the output radiation or reception intensity plotted as a function of the angles in which this intensity is directed [9]. The most basic radiation pattern is created by an isotropic radiating element, which is a hypothetical element that radiates equally in all directions. However, in practice every antenna radiation pattern, even the most basic, consists of more than one isotropic element [6].

Radiation Fields

The distance between the antenna and the intended receiver is an important parameter which determines the received signal strength. Based on this distance, there are three main regions in which antennas propagate electromagnetic waves differently: reactive near-field region, radiating near-field region, and far-field region as shown in Fig. 2.

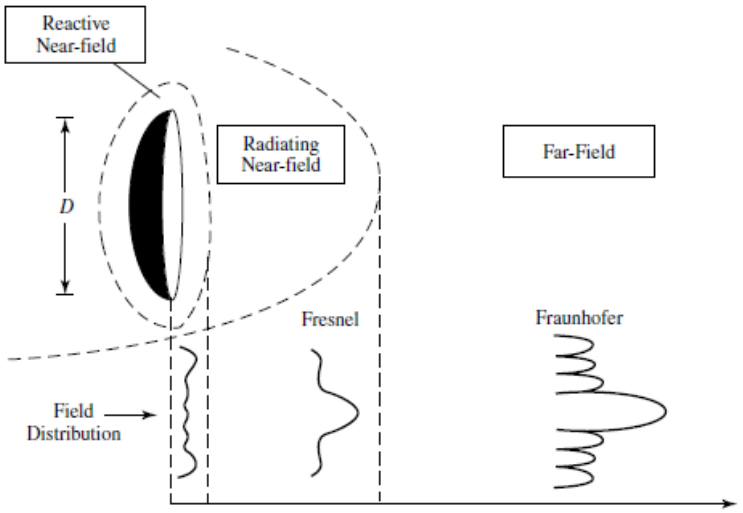

Fig. 2. The main three radiation fields [6]

The reactive near-field region is the space immediately surrounding the antenna, in which the reactive field predominates. In this region, a significant portion of the energy is stored and returned to the antenna [9]. The radiating near-field region or Fresnel region falls after the reactive near-field region and is characterized by radiation fields which dominate the reactive fields, and the angular distribution of this radiated field is dependent on the distance from the antenna [6]. Lastly the far-field region falls after the radiating near-field region, and is characterized as the space in which radiation is

essentially confined to a fixed pattern, and the power density along the axis of the pattern falls off inversely with the square of the distance [9]. In this region, the radiating field not only dominates the reactive field but also creates an angular field distribution which is not dependent on the distance from the antenna. In practice, the distance from the antenna to the receiver will almost always fall within the far field region. All of the patterns analyzed within this study are evaluated in the far field region.

The equations used to calculate the distances which separate the reactive near-field (r_{rnf}) region, radiating near-field (r_{Frs}) region, and far-field (r_{ff}) region are given below:

$$r_{rnf} \leq 0.62 * \sqrt{\frac{D^3}{\lambda}} \tag{1}$$

$$0.62 * \sqrt{\frac{D^3}{\lambda}} < r_{Frs} < \frac{2 * D^2}{\lambda} \tag{2}$$

$$r_{ff} > \frac{2 * D^2}{\lambda} \text{ [6].} \tag{3}$$

In these equations, D is the largest dimension of the antenna and λ is the wavelength of the wave.

Linear Phased Array Antenna

To obtain an understanding of a planar PAA, it is important to begin by describing the preliminaries, which focus on linear phased array configurations. Linear PAAs lay the

foundation for more complicated planar array structures. A linear antenna array consists of antenna elements which are distributed in a straight line.

For modeling the transmitting properties of a linear antenna array, it is more suitable to view the antenna as a receiving element rather than a transmitting element. This assumption does not add any complications because, by virtue of the reciprocity theorem, the characteristics of an antenna when used in transmitting are identical to those when used in receiving [6]. The simplest linear phased array antenna is composed of omnidirectional elements equally spaced along an axis. To analyze the properties of this antenna, it is first assumed that a source is transmitting an isotropic electromagnetic wave from the far field. In the far field, this wave acts as a plane wave as it reaches the antenna array. When the received plane wave is incident on the linear PAA, it will differ only by a phase difference at each element. This phase difference can be calculated according to Equation (4):

$$\Delta\varphi = x * k = x * \frac{2\pi}{\lambda} = dx * \sin(\theta) * \frac{2\pi}{\lambda}. \quad (4)$$

In this equation: $\Delta\varphi$ is the phase difference, x represents the extra distance the wave has to travel from one element to the next, k is the wavenumber (number of wavelengths per 2π radians), dx is the distance between two antenna array elements and θ is the direction of the incident plane wave. An illustration of these parameters can be seen in Fig. 3.

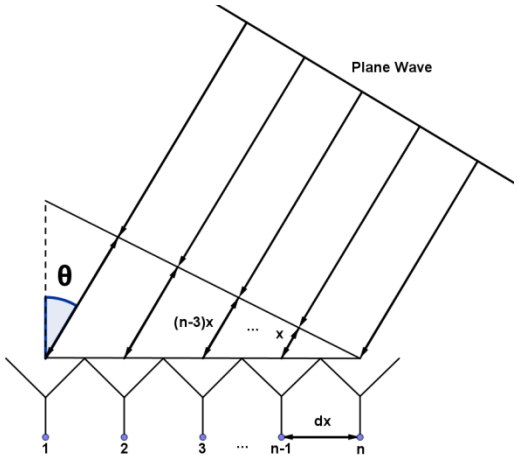

Fig. 3. An illustration of a linear PAA receiving a planar wave.

A sinusoidal wave is the most basic electromagnetic wave which can be received by each element and is represented in Equation (5).

$$s(t) = A * \cos(\omega * t \pm k * l) \tag{5}$$

In this equation, A is the amplitude of the signal, ω is the anglar frequency ($\omega = 2\pi f$ where f is the frequency of the signal), t is the elapsed time, k is the wave number, and l is the distance traveled.

Euler's formula is used to simplify the wave equation into an exponent as shown below.

$$s(t) = A * \cos(\omega * t \pm k * l) = A * Re\{e^{j(\omega * t \pm k * l)}\} \tag{6}$$

$Re\{*\}$ represents the real part of the equation; however, this notation is dropped in order preserve brevity.

As was mentioned previously, when the electromagnetic plane wave reaches each antenna element, the signal at each element will differ only by the phase difference calculated earlier. With this phase difference ($\Delta\varphi$), the signal ($s_i(\theta)$) at each element (i) as well as the total sum of all received signals ($S_a(\theta)$) from an array with N total elements can be obtained as follows.

$$s_i(\Delta\varphi) = \cos\big((\mathrm{N} - i) * \Delta\varphi\big) \tag{7}$$

$$s_i(\theta) = \cos\left((\mathrm{N} - i) * dx * \sin(\theta) * \frac{2\pi}{\lambda}\right) \tag{8}$$

$$s_i(\theta) = e^{(\mathrm{N}-i)*j*dx*\sin(\theta)*\frac{2\pi}{\lambda}} \tag{9}$$

$$S_a(\theta) = s_1(\theta) + s_2(\theta) + \cdots + s_{N-1}(\theta) + s_N(\theta) \tag{10}$$

$$S_a(\theta) = \sum_{i=1}^{N} e^{(\mathrm{N}-i)*j*dx*\sin(\theta)*\frac{2\pi}{\lambda}} \tag{11}$$

A unitary amplitude (*A=1*) is assumed for brevity.

These results can be reversely applied to transmitting antennas. To achieve an optimal radiation pattern, the fields from each the antenna elements need to interfere positively (constructive interference) in the desired direction and have negative interference in all other directions (destructive interference). This can be achieved by applying the phase shifted radiation pattern described above to each antenna element. As such, the far field

radiation pattern from an N-element linear and equally spaced array is a summation of the radiation of each element according to the equation below Equation (12):

$$E(\theta, \phi) = \sum_{n=1}^{N} E_n(\theta, \phi) * e^{j*k*n*d*\sin(\theta)} \quad (12)$$

where $E_n(\theta, \phi)$ is the electric field pattern of each element (n), j is the imaginary unit, and k is the wave number ($2\pi/\lambda$). Furthermore, d represents the distance between two elements (dx in Fig. 3. and Equation (4)) while θ is the angle of the incident wave.

Assuming that all the patterns produced by the antenna are identical, the equation for the summed radiation pattern can be rewritten and divided into two parts, the element pattern and the array factor, as shown below Equation (13).

$$E(\theta, \phi) = \underbrace{E_{ele}(\theta, \phi)}_{Element\ Pattern} * \underbrace{S_a(\theta)}_{Array\ Factor} \quad (13)$$

where

$$S_a(\theta) = \sum_{n=1}^{N} e^{j*k*n*d*\sin(\theta)} \quad (14)$$

In practice, the element pattern (E_{ele}) describes the radiation of a single antenna element and will therefore be different depending on what kind of antenna element is used [10]. The array factor (S_a) is dependent on the number of antenna elements in the array (N), the wave number ($k=2\pi/\lambda$), the element spacing (d), and the incident angle of the wave (θ) [11].

Simplifying the Array Factor

As shown in the previous section, the array factor is given by Equation (14), yet this equation can further be simplified as shown in [6]. Following these simplifications, the results below are obtained,

$$S_a(\theta) = \sum_{i=1}^{N} e^{j*k*(N-i)*d*\sin(\theta)} = \sum_{i=1}^{N} e^{j*(N-i)*T} \tag{15}$$

where

$$T = k * d * \sin(\theta). \tag{16}$$

Equation (15) is a finite geometric series, and if multiplied by e^{j*T} on both sides the following series is obtained,

$$S_a(\theta) * e^{j*T} = e^{j*N*T} + e^{j*(N-1)*T} + \cdots + e^{j*2*T} + e^{j*T}. \tag{17}$$

After a subtraction between the series above and $S_a(\theta)$, the following is obtained

$$S_a(\theta) * \left(e^{j*T} - 1\right) = \left(e^{j*N*T} - 1\right) \tag{18}$$

This equation can further be simplified to

$$S_a(\theta) = \frac{e^{\frac{j*T}{2}} * \left(e^{j\frac{N*T}{2}} - e^{-j\frac{N*T}{2}}\right)}{e^{j\frac{N*T}{2}}\left(e^{j\frac{T}{2}} - e^{-j\frac{T}{2}}\right)} = e^{j\frac{(N-1)}{2}*T} * \frac{\sin\left(\frac{N}{2} * T\right)}{\sin\left(\frac{1}{2} * T\right)} \tag{19}$$

and finally

$$|S_a(\theta)| = \left|\frac{\sin\left(\frac{N}{2} * k * d * sin(\theta)\right)}{\sin\left(\frac{N}{2} * k * d * sin(\theta)\right)}\right| = \left|\frac{\sin\left(\pi * \frac{N * d}{\lambda} * sin(\theta)\right)}{\sin\left(\pi * \frac{d}{\lambda} * sin(\theta)\right)}\right|. \tag{20}$$

Antenna element spacing plays a vital role in the coupling of the electric fields. As the element spacing increases, so does the directivity of the antenna. However, to some extent, the element spacing will also cause an increase of side lobes and grating lobes in the radiation pattern, as is shown in the next sections: *Side Lobes* and *Avoiding Grating Lobes*.

Planar Phased Array Antenna

Planar antenna arrays are composed of antenna elements which are spread across a two dimensional plane, and can be described as a linear array of linear antenna arrays. Each element of the array has a horizontal and vertical spacing between its neighbors. Planar arrays can have numerous geometric structures and can be very complex. However, for simplicity a planar array with equidistant elements in both the horizontal and the vertical direction is introduced. An illustration of a planar phased array antenna is shown in Fig. 4.

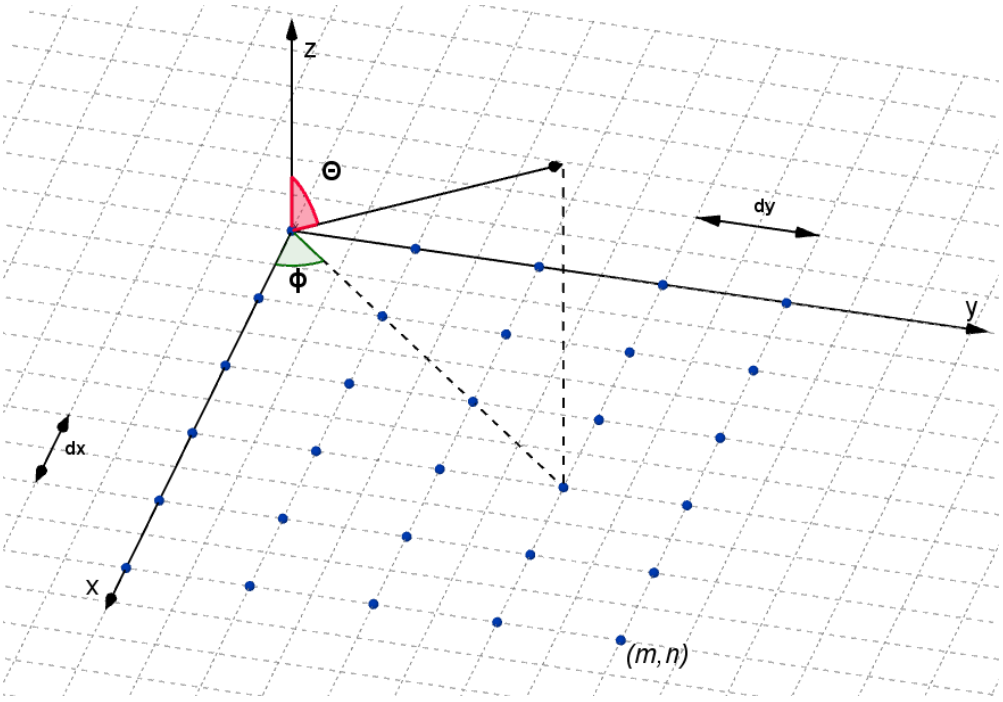

Fig. 4. An illustration of a planar phased array consisting of m by n elements, having spatial differences of dx units horizontally and dy units vertically. The beam formed by this array is pointed in the (θ, ϕ) direction where ϕ represents the azimuthal angle, and θ represents the elevation angle.

The radiation field from a planar array is a summation of the radiation from each element, just like for the linear array. Because the planar array is distributed over two dimensions, as the plane wave is incident on each antenna element, the wave will differ only by a phase difference which is based on both *theta* (θ) and *phi* (ϕ). The phase difference is shown to be as below [6].

$$\Delta\varphi = k * \sin(\theta) * (m * dx * \cos(\phi) + n * dy * \sin(\phi)). \qquad (22)$$

When this phase difference is introduced in every pattern the total radiated electric field is represented according to Equation (22).

$$E(\theta,\phi) = \sum_{m=1}^{M}\sum_{n=1}^{N} E_{ele}(\theta,\phi)e^{j*k*\sin(\theta)*(m*dx*\cos(\phi)+n*dy*\sin(\phi))} \quad (22)$$

This equation can be rewritten as

$$E(\theta,\phi) = E_{ele}(\theta,\phi) * S_{a1}(\theta,\phi) * S_{a2}(\theta,\phi) \quad (23)$$

where

$$S_{a1}(\theta,\phi) = \sum_{m=1}^{M} e^{j*k*m*d*\sin(\theta)*\cos(\phi)} \quad (24)$$

$$S_{a2}(\theta,\phi) = \sum_{n=1}^{N} e^{j*k*n*d*\sin(\theta)*\sin(\phi)}. \quad (25)$$

$\boldsymbol{E}_{ele}$ indicates the element pattern, *k* the wave number and *dx* and *dy* respectively represent the distance between two elements in the x and y directions. By utilizing a planar array, the main beam can be directed in two dimensions and further controlled in both the θ and ϕ directions. For better representation, radiation patterns can be transformed in multiple ways. As an example, plotting the pattern in the *uv* plane requires a change of variables utilizing Equation (26) and Equation (27) below

$$u = \sin\theta * \cos\phi \quad (26)$$

$$v = \sin\theta * \sin\phi \quad (27)$$

Radiation Pattern of Antenna

In obtaining the radiation pattern of the PAA, each element is modeled as emitting hemispherical isotropic radiation similar to Fig. 5. A hemisphere rather than a sphere is taken into account in order to decrease the computational load by eliminating the back side of the pattern. This part of the pattern is not used in calculating frontal beam formations.

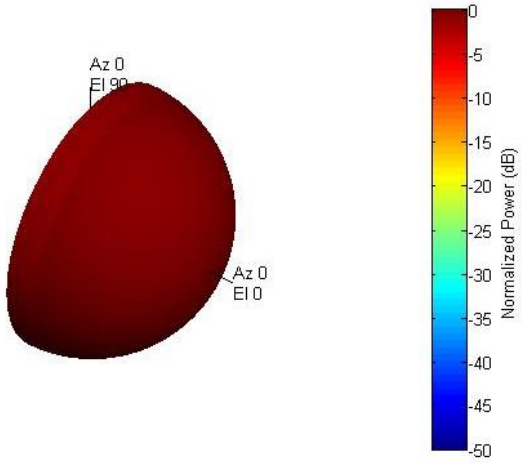

Fig. 5. Radiation pattern of an isotropic antenna element in the far field.

Using the phases calculated in Equation (21), at a desired direction, the radiation pattern of the 2 x 8 and 4 x 4 array configurations are obtained. An example of these patterns is displayed in Chapter IV.

Side Lobes

When the array pattern is used as a transmitter, the elements in this scenario radiate rather than intercept electromagnetic radiation. The mathematical representation of this radiation is the same as depicted in Equation (22). With this equation, several properties of the radiation pattern can be analyzed. Side lobes and grating lobes are of significant interest. Side lobes, as their name indicates, are maxima in the radiation pattern other than the main lobe [9]. When transmitting a signal to one intended user, side lobes are undesirable for several reasons. First, side lobes radiate energy in undesirable directions, thus they are wasteful in the transmitting of information. Furthermore, this radiation, if excessive can, not only cause interference in transition, but may also be picked up by unintended users. The most prominent of side lobes are grating lobes.

Avoiding Grating Lobes

A radiation pattern has a main beam which points in a specific direction. However, under certain circumstances the radiation pattern of an antenna array can constructively interfere to form an equally strong radiating beam in another direction. These sometimes undesirable lobes are known as grating lobes [9].

To avoid the occurrence of grating lobes, the element spacing must be set strategically. This can be done by analyzing the mathematical representation of the array pattern, and extracting the locations at which elements do not create grading lobes. To determine the

optimal element spacing for a linear phased array antenna, a step by step guide of this process is shown below [6].

The array factor calculated previously for a linear phased array is revisited:

$$|S_a(\theta)| = \left| \frac{\sin\left(\pi * \frac{N * d}{\lambda} * sin(\theta)\right)}{\sin\left(\pi * \frac{d}{\lambda} * sin(\theta)\right)} \right|. \quad (28)$$

In this equation, θ is the angle of the main beam, d is the distance of element spacing, and λ is the wavelength of the transmitting signal. Equation (28) can be simplified

$$|S_a(\theta)| = \left| \frac{\sin(N * x)}{\sin x} \right| \quad (29)$$

where

$$x = \pi * \frac{d}{\lambda} * sin(\theta). \quad (30)$$

It can be observed that the array factor is at a maximum when $x = \pi$ in the above equation, or periodically when

$$\pi * \frac{d}{\lambda} * sin(\theta) = m * \pi \quad (31)$$

for m =1, 2, 3, …

The distance of element spacing can be solved for by simplifying the above equation as follows:

$$d = \frac{m * \lambda}{sin(\theta)}. \quad (32)$$

The focus is only on obtaining one main beam, utilized to communicate with one user. Thus, the optimal scenario is for the antenna to generate one main lobe and no grating lobes in the radiation pattern. The beam should be able to move the main lobe in the visible space (from +90 to -90 degrees azimuthal angle range) without any grating lobes arising.

With these requirements, the optimal element spacing for the uniform linear array antenna is

$$d \leq \lambda. \quad (33)$$

This was obtained utilizing m=1 thus limiting the development of one main lobe and no extra grating lobes to follow, and $\theta = \frac{\pi}{2}$ for limiting the scanning range as previous discussed. However, these results are only valid when the beam is at broad side and unfortunately do not tell the full story of how grading lobes will arise if the main lobe is moved to other locations. In this case, one needs to look at the addition of a phase factor (α) in Equation (34) as follows,

$$T = k * d * \sin(\theta) - \alpha \quad (34)$$

This changes the array from Equation (15) to

$$S_a(\theta) = \sum_{n=1}^{N} e^{j*n*(k*d*\sin(\theta)-\alpha)}. \quad (35)$$

This equation forms maxima when $T = n * 2 * \pi$. More specifically, for one maximum T=0 and for placing the maximum at endfire $\theta = 90°$. With these variables the additional phase factor is

$$\alpha = -k * d. \quad (36)$$

This factor can allow us to observe multiple grating lobes occurring when

$$T = k * d * \sin(\theta) + k * d = n * 2 * \pi \quad (37)$$

$$k * d * (\sin(\theta) + 1) = n * 2 * \pi \quad (38)$$

$$d = \frac{\lambda}{\sin(\theta) + 1} \quad (39)$$

For placing the beam at a maximum angle of $\theta = 90°$,

$$d = \frac{\lambda}{2} \quad (40)$$

Thus, when the elements have a spacing of approximately $d \leq \frac{\lambda}{2}$, it is possible to theoretically design a uniformly linear array antenna to scan from +90° to -90°. These results can be used to dictate the rectangular PAA element distances as well. However, in practice the radiation impedance changes with each scan and severely caps the scan angle to a range of around +60° to -60° [10].

Beamwidth

A phased array's element spacing not only influences the occurrence of side lobes but also influences the beamwidth of the radiation pattern. The beamwidth or half power beamwidth of a radiation pattern is the angle between the half power (-3 dB) points of the main lobe [9]. Another factor that influences the directivity and beamwidth of the radiation pattern is the number of elements used to construct the antenna. This section analyzes the effects the number of elements has on a linear phased array with equal element distances.

The beamwidth of a phased array can be wide and can cover a larger area; however, in most cases a narrow beamwidth is more favorable in order to obtain a strong connection with a user at a known location. To decrease the beamwidth of a phased array antenna, one can increase the directivity of every antenna element, increase the amount of elements used in the array, or decrease the distance between elements.

Assuming that in a linear phased array an optimal element distance is set and that the array elements are kept as isotropic radiators, the only parameter which can further be adjusted to improve the beamwidth is the number of elements.

In determining how many elements to use in the construction of the phased array, it is important to decide on the beamwidth of the array or empirically determine a favorable beamwidth. However, increasing the number of elements to attain a better resolution and

smaller beamwidth will come at the cost of complexity and added expenses. An ideal is to minimize the beam width while at the same time keeping the cost and complexity of the antenna within reasonable thresholds.

It can be shown that for a beam scanned at angle θ_0, the 3-dB-beamwidth $\theta_3$is given by [12].

$$\theta_3 = \arcsin\left(sin\,\theta_0 + 0.4429 * \frac{\lambda}{N * d}\right) - \arcsin\left(sin\,\theta_0 - 0.4429 * \frac{\lambda}{N * d}\right). \quad (41)$$

Furthermore, the 3 dB beam collapse angle is also impacted by the number of elements of the array. The 3 dB beam collapse angle, or the angle at which the main beam's 3 dB beamwidth hits the ±90 degree threshold, occurs at larger angles in phased arrays having more elements. A large 3 dB beam collapse angle is desired in order to retain resolution of the main beam. The 3db beam collapse angel can be used to determine the number of array elements to be used and can be obtained through Equation (42) [12]

$$\theta_0 = \arcsin\left(1 - 0.4429 * \frac{\lambda}{N * d}\right). \quad (42)$$

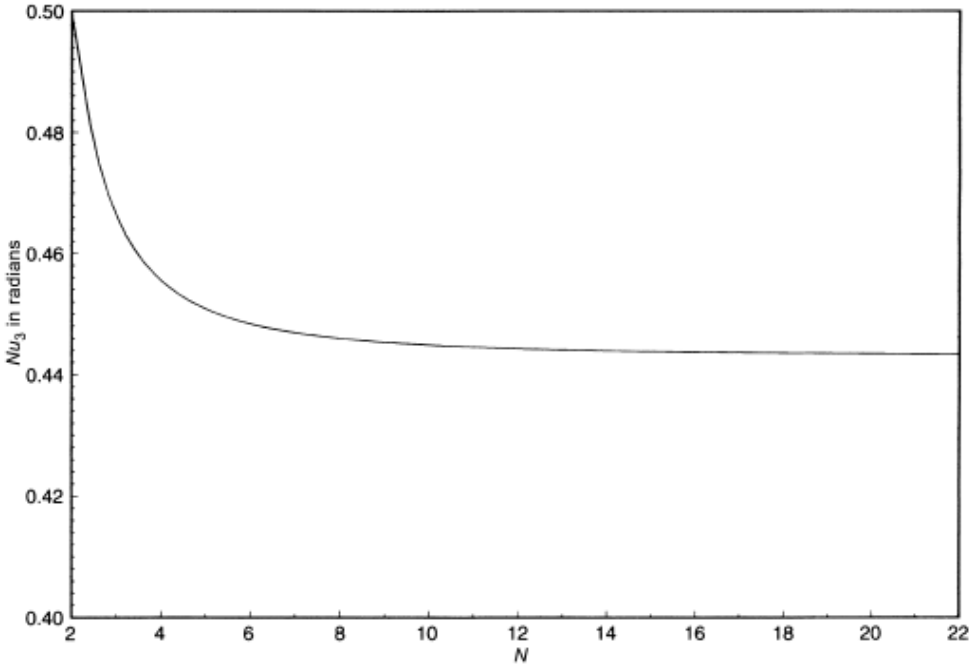

Fig. 6. Normalized beamwidth versus number of elements [12].

Plotting the previous equations a threshold can be observed when looking at Fig. 6. and Fig. 7. Therefore, the number of elements to be used in the array can be selected based on required parameters in beamwidth and 3 dB beam collapse angle.

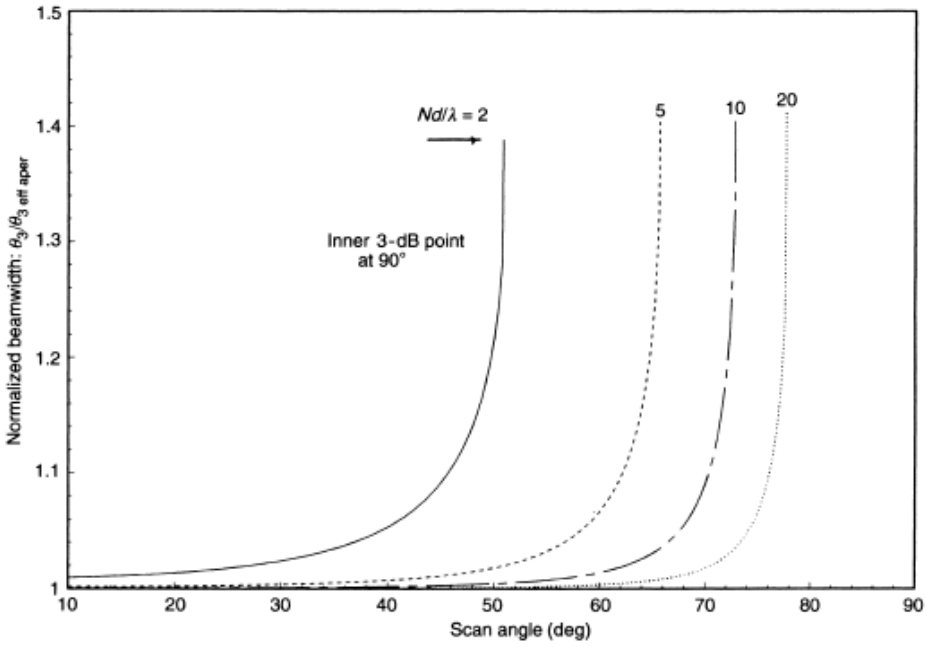

Fig. 7. Beamwidth broadening versus scan angle [12].

Quantifying Uplink and Downlink

To determine the way phased array antennas can transmit, it is important to analyze the uplink and downlink capabilities of each antenna. Uplink is defined as the radio frequency link from a site on earth (user) to a satellite or base station (beacon) [9]. Downlink is defined as the radio frequency link from a satellite or base station (beacon) to a site on earth (user) [9]. A graphical representation is shown in Fig. 8.

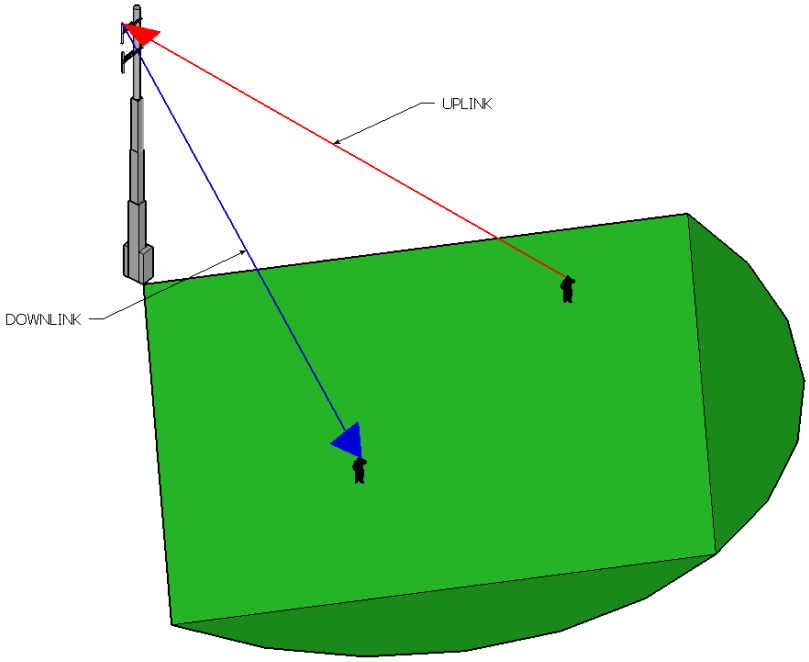

Fig. 8. The uplink and downlink from base station to user.

In quantifying the uplink and downlink performance of each antenna, an analysis on the way the signal models on the desired area is conducted. In doing so, the signal strength is analyzed in relation to the location of the intended receiver. By looking at how the signal strength varies, the antenna which performs best in the given scenario can be identified.

To determine the superiority of one phased array structure over the others, several parameters can be observed and analyzed. Two of these parameters are the statistical expectation and variance. More specifically, they are the expectation and variance of the received signal strength and the expectation and variance of the interference given the

location of the receiver. These parameters play an important role in analyzing the efficiency of the downlink and uplink between the user and the antenna. They are fundamental factors which will be used to determine the superiority of one antenna configuration over the others.

Free Space Path Loss

As the signal from and to the antenna propagates through space, it incurs losses based on several factors. Numerous models, which account for environmental factors, exist to accurately explain the way the signal propagates. A model which is frequently considered in this analysis is the free space path loss formulation. As defined, the free space path loss is the loss in signal strength of an electromagnetic wave that would result from a line of sight path through free space (usually air) with no obstacles nearby to cause reflection or diffraction [13]. The free space path loss is proportional to the square of the distance between the transmitter and receiver [13]. In this study, the path loss was modeled with a distance dependency. Distance decay is caused by the spreading out of electromagnetic energy in the free space and is described by the inverse square law [13].

$$S(d) = P_t * \frac{1}{4 * \pi * d^2} \tag{43}$$

where *S(d)* is the power per unit area or power spatial density (in watts per meter-squared) at distance *d*, P_t is the equivalent isotropic radiated power (in watts). Succinctly, in comparing the transmitted power and the received power, the received

power is inversely proportional by the square of the distance between the transmitter and receiver.

Downlink

Because the tower antenna (beacon) is designed to propagate and receive signals from large distances, the transmitted signal is more powerful than a received signal. In rare situations the transmitted signal incurs distortion or interference from neighboring antenna towers. Because of this, the downlink can purely be quantified by the expectation of the received signal from the tower to all user locations in the area.

To analyze the downlink, the signal strength from the antenna to receiver is modeled. The free space path loss formulation, as well as the configuration of each antenna is used in determining the signal received by the user. To calculate the optimal signal received by the user from the antenna tower, the following equation is utilized:

$$R(location_i) = T(location_i, Antenna) * FSPL(location_i). \quad (44)$$

In this equation, *R* represents the signal strength at $location_i$, which is the location of the receiver in the area, *T* represents the transmitted signal strength directed at $location_i$ and is a function of $location_i$ and *Antenna,* which represents the configuration of the antenna analyzed. Lastly *FSPL* is the free space path loss which is a function of the distance between the antenna tower and $location_i$. After the received signal for each location is calculated, the expectation and variance of a finite discrete random variable, is calculated.

The expectation of the received signal for all receiver locations can be computed as follows:

$$E[R] = R_1 p_1 + R_2 p_2 + \cdots + R_k p_k. \quad (45)$$

In this equation, $R_1, R_2, \ldots, R_k$ are the values representing the received signal strengths at the corresponding *location*$_1$, *location*$_2$ *…location*$_k$ (calculated in Equation (44)), and $p_1, p_2, \ldots, p_k$ are the values representing the probabilities of the received signal strengths. Assuming that the user is equally likely to be anywhere in the area, the probabilities of the received signal strengths is shown in Equation (46):

$$p_1 = p_2 = \cdots = p_k = \frac{1}{Area\ of\ sector} = c. \quad (46)$$

This simplifies Equation (45) to

$$E[X] = (R_1 + R_2 + \cdots + R_k) * c. \quad (47)$$

The variance of the received signal for all receiver locations can be computed as follows:

$$Var[X] = E[(R_i - E[X])^2]. \quad (48)$$

Uplink

In relation to the signal strength of the downlink (from beacon to user), the signal strength of the uplink (from user to beacon) is less powerful. For this reason, attenuation and interference can impact this signal in numerous ways. Thus, rather than follow the signal from the user to the antenna tower on the uplink, the signal from the tower to the user is analyzed similar to the downlink. This procedure can be followed by using the

law of reciprocity. Therefore, the way the signal models from the base station to the user is the same if the antenna elements are phase-shifted ideally. The signal with highest strength from the user to the beacon will be the same as a signal with the highest strength from the beacon to the user.

However, to determine the performance of each antenna on the uplink, the signal expectation and variance is analyzed based on interference. By doing so, the expectation of the interference is modeled as follows:

$$E[X|location\ of\ x_i] = [(x_1 + x_2 + \cdots + x_k) - x_i] * c_A, \tag{49}$$

where $c_A = \frac{1}{Area\ of\ sector - \frac{k-1}{k}} \approx c$.

This equation is used to compute the expectation of interference given the location of the user. In this scenario, the beam of the antenna is directed towards the user's location so she can obtain maximum signal strength. All other transmitted power is considered interference: $x_1, x_2 \ldots x_k$. The transmitted power for each point in the area is calculated, summed, and divided by the area of the sector, in order to obtain the expectation of the interference for every receiver location.

In computing the variance of the interference, the law of total variance is used. From the literature, total variance is expressed as:

$$Var(X) = \underbrace{E[Var(X|Y)]}_{1} + \underbrace{Var(E[X|Y])}_{2}. \tag{50}$$

The equation is broken down into two parts.

1) The expected value of the conditional variance:

$$E[Var(X|Y)] \tag{51}$$

2) The variance of the conditional means:

$$Var(E[X|Y]). \tag{52}$$

X is taken to be the random variable representing the signal strength observed by the user. Y is taken to be the random variable representing the location of the user in the area.

To compute Equation (51), the following equations are used:

$$E[X] = (x_1 + x_2 + \cdots + x_k) * c\ . \tag{53}$$

$$Var[X] = E[(R_i - E[X])^2] \tag{54}$$

Equation (51) can be seen as the weighted average of Var(Y|X).

To compute (52), the following equation for variance is used

$$Var(E[X|Y]) = E\left(\left[E(X|Y) - E\left(E(X|Y)\right)\right]^2\right) = E([E(X|Y) - E(X)]^2) \tag{55}$$

This equation can be seen as the weighted average of $[E(X|Y) - E(X)]^2$.

To note, the distribution of transmitted signal strength from the antenna and received signal strength to the users in the geographical area acts as random variables. The

position of the user can be randomly distributed across the area, and the transmitted power to the user is the random property to be analyzed. The transmitting power is determined by the user's location, and is defined on a sample space with a maximum and minimum value.

CHAPTER III

SYSTEM MODEL

Study of Area

To properly design a phased array antenna intended to communicate with a user, a first step is to analyze the area in which the antenna is to operate. This area will impact the size, shape, configuration, and power of the phased array. In this study, the setting of the antenna is an outdoor environment, which does not create any geographical interference between the antenna and the receiver. The area is sectioned in hexagonal cells as shown in Fig. 9. This is typical of the methodology used for performance analysis in cellular systems [14].

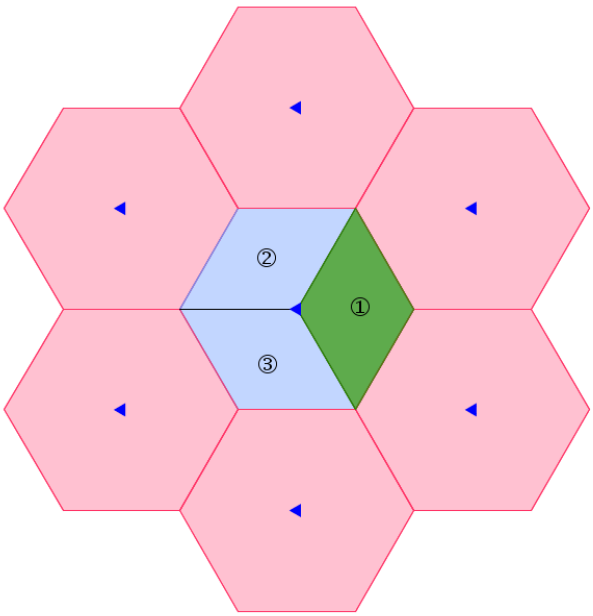

Fig. 9. Splitting the area into hexagonal cells

In practice, cellular telephone systems implement cell sites which are grouped in areas of high population density, with the most potential users. In suburban areas, cell phone towers are commonly spaced 1 to 2 miles (2 to 3 Km) apart and in dense urban areas, they can be as close as a quarter to one half of a mile (400–800 m) apart [15]. Taking these parameters into account, we decided that the area of study is to be split into regular hexagonal cells having side length of 1 mile (~1.6 Km). With this cell length, the towers are spaced 1.732 miles away and ideally represent a rural environment covering a flat area.

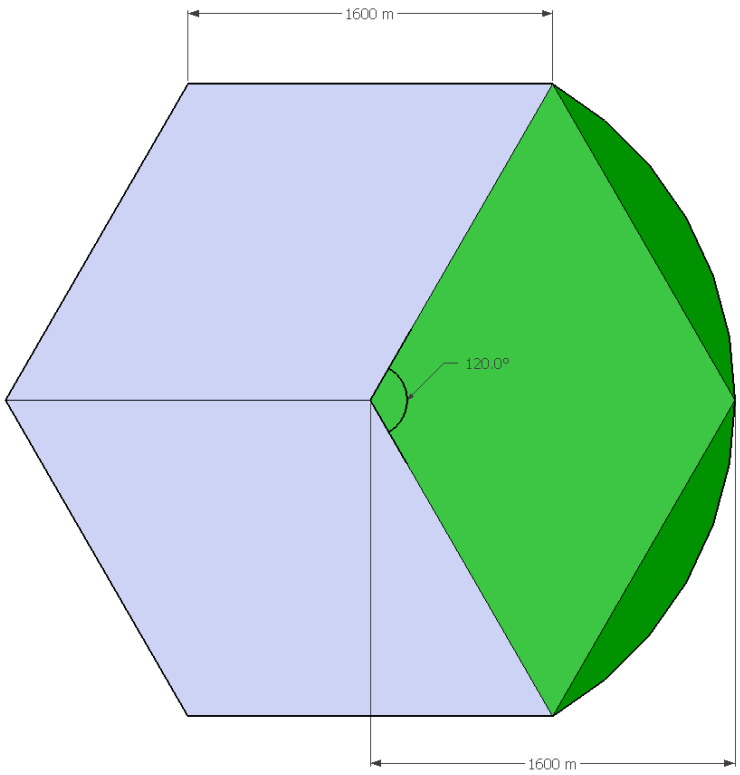

Fig. 10. Sectioning of each cell into three identical portions.

The cell is further sectioned into 3 equal parts, as is shown in Fig. 10. An antenna tower is located in the center of each cell and at the top of each tower three identical phased arrays are placed, each one facing the section it is assigned. Only one section is analyzed because of the symmetry in this system.

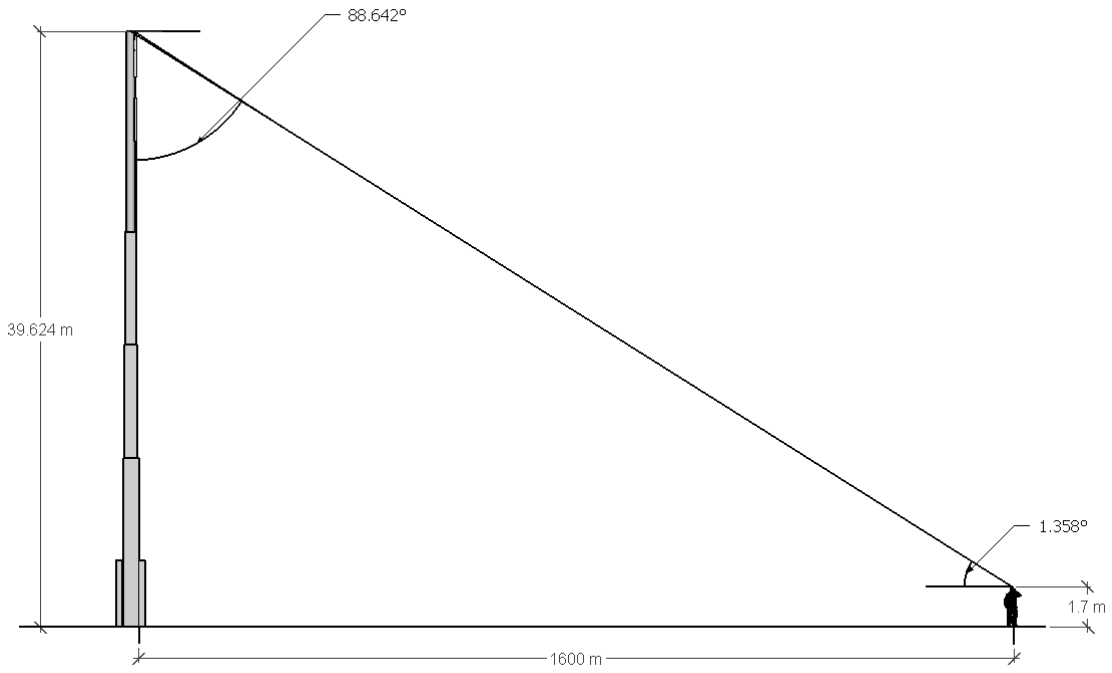

Fig. 11. Side view of furthest receiver away from the antenna. *Not to scale.

In deciding the height at which to place the phased array a study of FCC records in 2012 was analyzed. The study showed that the most prevalent cell phone tower height in the United States ranges from 100 feet to 350 feet [16]. However because the area covered by the antenna is idealized and does not contain any geographical structure to inhibit line of sight, we set the height of the tower to a conservative 130 feet (39.624 m). The

intended receiver to which the antenna transmits information was decided is a mobile device. The mobile device is to be used by a person as shown in Fig. 11. The height at which the mobile device is placed is 5 feet 7 inches (1.7 m) or the average height of an American based on a 2003-2006 census [17]. The largest distance which the signal will have to travel is the hypotenuse formed by the height of the cell tower (39.624 m) minus the height of the user (1.7 m) and the radius of the cell (1600 m). This setup is show in Fig. 11. and Fig. 12.

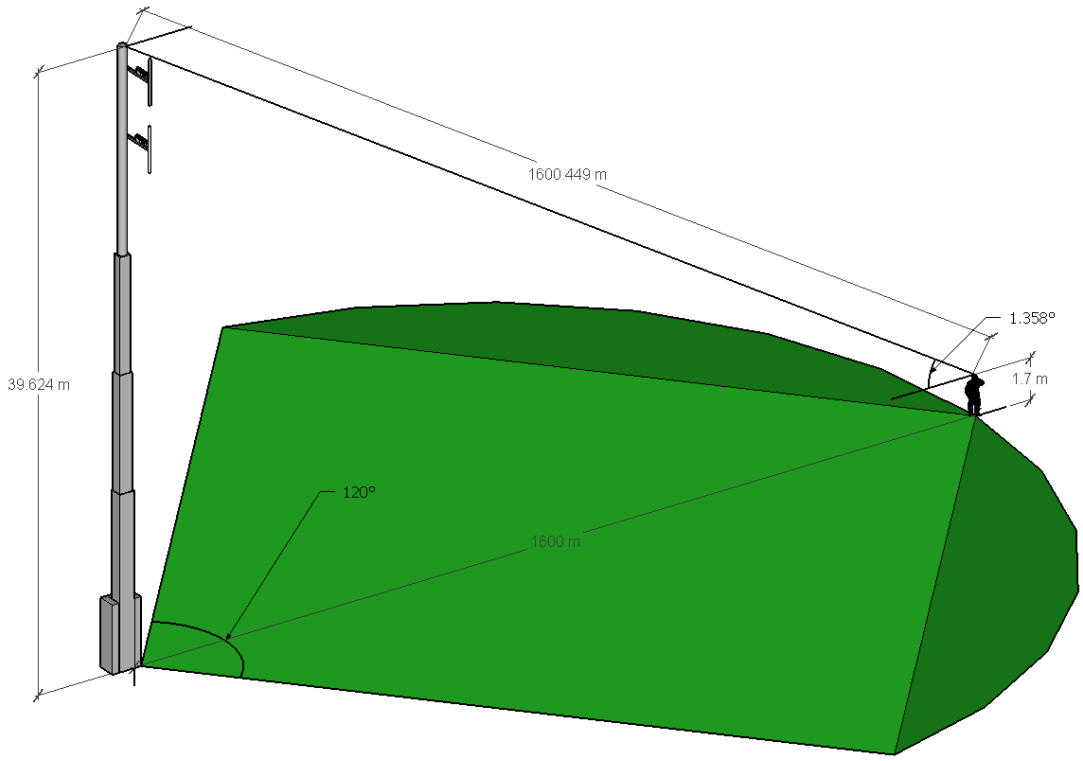

Fig. 12. 45 degree view of furthest receiver away from the antenna. *Not to scale.

Receivers in the Area

After the area was determined, the placement and location of the receiver was analyzed. To model the locations at which receiver can be situated, the area is sectioned off into a grid with the grid nodes representing receivers. Although the grid encompasses half of the hexagonal cell, only receivers located in the primary sector are of interest. The grid size utilized is 50 by 50 totaling 2500 points. As can be seen in Fig. 13., the grid points are not equidistant in the *x* and *y* direction. There are 50 points equally spread on the x axis from the center to the middle vertex of the hexagon, and there are 50 points equally spread from the top edge to the bottom edge of the hexagon. Thus the points on the *x* axis are more tightly backed than those on the y axis. Grid points within the rhombus, the area of interest, are colored red those outside are blue. These red grid points represent specific locations at which the radiation patterns of each antenna will be analyzed. However, for some receiver locations the radiation pattern cannot be directly mapped and an interpolation of these radiation values is used. There are 1200 total

Proposed Antenna

Element Properties

Any antenna element can be used in the construction of a phased array. Yet, the antenna elements which are chosen have certain repercussions on the entire array. The element properties not only have a huge impact on the directivity of the array beam but also receiver locations within the area of interest.

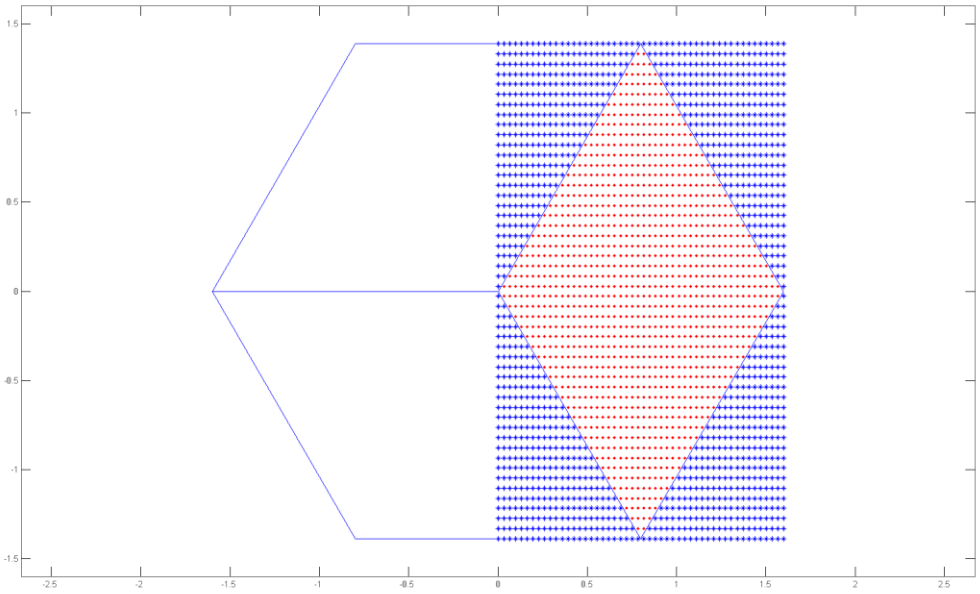

Fig. 13. Hexagonal cell with radius of 1600 meters (1 mile) sectored in 3 equal rhombus areas. Half of the hexagonal cell is divided by a 50 by 50 grid. Grid points within the rhombus, the area of interest, are colored red those outside are blue. The red grid points represent specific locations at which the radiation patterns of each antenna will be analyzed. There are 1200 total red points.

determine the arrays size and complexity. In addition, element properties also establish the transmitting frequency of the antenna which directly relates to the antenna wavelength. Furthermore, depending on the number of elements used, the replication of each element, if not exact, can cause imperfections in the beam produced. Ideally, the elements used should have high directivity or high gain and a small footprint. In this study, omnidirectional point source elements were used. With these elements the computation of the array pattern follows the general theory discussed in Chapter II, thereby, eliminating the computational complexity of the radiation pattern at the expense of creating a wider output beam. After defining the element properties, the next step is to determine the total number of elements to use for the array.

Element Number: 16

As discussed in Chapter II, the number of elements to be used in constructing a phased array is one of the most significant variables to consider because it influences cost, size (antenna aperture), directivity (side lobes and beamwidth), and complexity (phase shift calculations). After taking these parameters into consideration, the number of antenna elements to be used in this study was chosen to be 16. This number is selected for several reasons. First, with 16 elements, a linear phased array antenna can be constructed having a resolution and beam width which falls within acceptable boundaries as shown in Chapter II (Fig. 6.). In addition, 16 elements can be configured in numerous ways to create multiple antennas with large aperture sizes. Due to these observations, 16 elements were utilized in the simulation of 3 phased array antennas. With the element number defined, the next design parameter which is discussed is the arrangement of the elements.

Arrangement of Elements

After the amount of elements (16) was chosen, the shape of the PAA is the next feature which needs to be analyzed. The shape of the antenna can have a dramatic impact on how the radiation pattern forms. For example, an array with more antenna elements placed on the horizontal axis rather than the vertical axis will have more accuracy shifting its beam horizontally as opposed to vertically. Phased array antennas can be constructed in several shapes, with the most common being rectangular, circular, or

triangular. Previous work has been done in determining the benefits of each geometric arrangement; in this study, a rectangular configuration was utilized.

Rectangular Geometry

A rectangular antenna configuration has certain benefits which made this configuration a final candidate in this study. The most beneficial aspect of the rectangular configuration is that it is easy to construct and follows the general theory discussed in Chapter II. This pattern also adds symmetry, as displayed in Fig. 14.; symmetry can eliminate some of the complexity in the beam construction. Furthermore, with this configuration, the side lobes as well as grading lobes can accurately be predicted and avoided. The three rectangular arrays constructed from 16 elements are the 4 by 4, 2 by 8 and 1 by 16. These antenna patterns were analyzed using a same procedure.

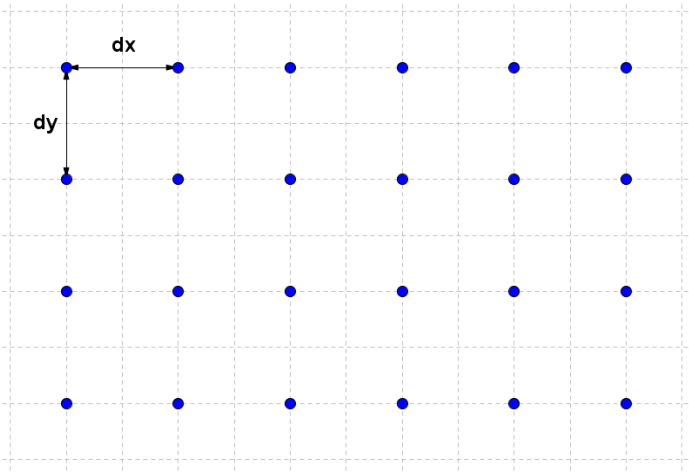

Fig. 14. Rectangular configuration of antenna array elements. Variable dx represents the horizontal element spacing and dy represents the vertical element spacing.

Antenna Element Distance

Side Lobe and Grating Lobes

With a rectangular array the side lobes and grating lobes created by the pattern can easily be determined using the equations in Chapter II. It was shown that with an element distance of $\frac{\lambda}{2}$, the grating lobes are eliminated from the field of view of a square lattice phased array antenna. A graphical representation of this concept is shown in Fig. 15.

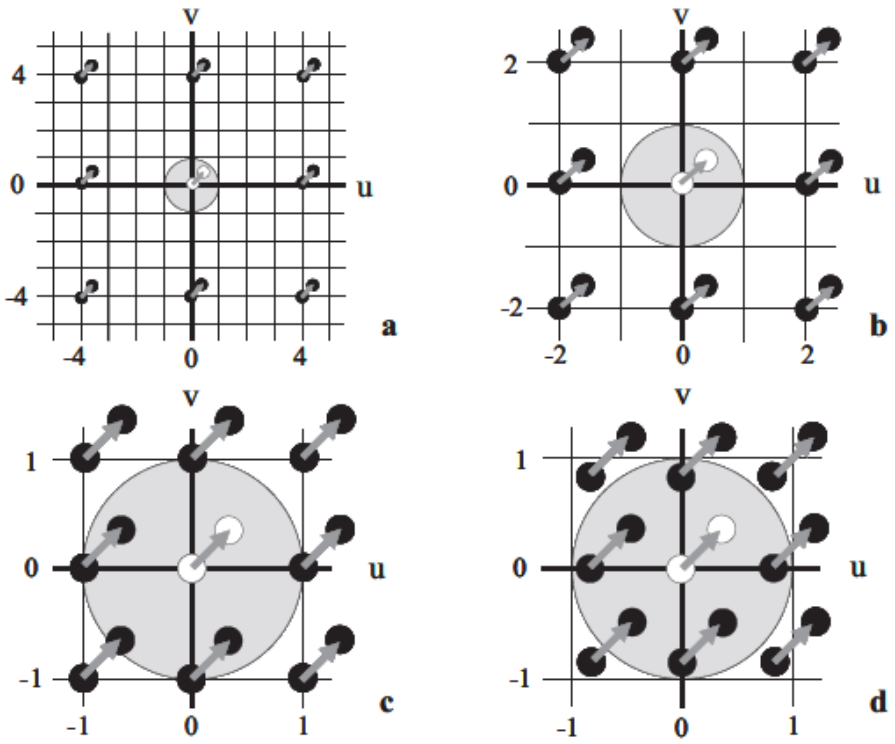

Fig. 15. Movement of grating lobes in Phase Array Antennas having different element spacing. [6]

In this figure, the white circle represents the main beam while the black circles represent the grating lobes. The gray circle represents the main field of view while the white space

represents the imaginary space. If the grating lobes are within the field of view, then they also protrude the antenna radiation pattern. If they are within the imaginary space, they are not apparent in the antenna radiation pattern. The translation of the beam and grating lobes is represented by the arrow in the figure. Ideally, the element spacing should be as large as possible in order to increase the aperture of the antenna and directivity of the main beam, while at the same time be able to keep any grating lobes from entering the field of view as the main beam is shifted within this view [6].

The configurations modeled in Fig. 15. are those having element spacing:

a) $dx = dy = \frac{\lambda}{4}$, b) $dx = dy = \frac{\lambda}{2}$, c) $dx = dy = \lambda$ and d) $dx = dy = \frac{5*\lambda}{4}$. The diagram directly shows that phased arrays (*a* and *b*) with element spacing $(dx = dy) \leq \frac{\lambda}{2}$ are able to keep grating lobes from entering the main field of view as the main beam is shifted. In contrast, phased arrays (*c* and *d*) cannot keep grading lobes from within the field of view regardless of where the main beam is positioned. These results directly correlate with the theory in Chapter II and show that the largest element spacing, which prevents grating lobes from entering the field of view, is $\frac{\lambda}{2}$. Furthermore, these results can be extended to any square lattice phase array regardless of its number of elements because the number of elements does not influence the position of the grating lobes, rather it affects the beam width and radiation strength of these lobes.

Wavelength

The wavelength used in this study is a function of the frequency with which the antenna transmits and receives. This transmitting frequency, as was introduced in Chapter I, is based on the 802.11 Wi-Fi protocol. It was chosen to be 2.5 GHz for this study. With this frequency set the wavelength is computed with the wave equation:

$$c = f * \lambda \tag{56}$$

in which c is the speed of light, f is the frequency, and λ is the wavelength.

Array Configurations

After establishing all the necessary properties: shape of elements, number of elements, arrangement of elements, element distances, and wavelength, the 3 array configuration can now be constructed. The three array configurations which were chosen are:

1) 1 by 16 linear pattern

   (59.958mm element spacing, 959.336mm aperture)

2) 2 by 8 square planar pattern

   (59.958mm element spacing, 479.668mm by 119.917mm aperture)

3) 4 by 4 square planar pattern

   (59.958mm element spacing, 238.834mm by 238.834mm aperture)

These structures can be seen in Fig. 16., Fig. 17. and Fig. 18.

1 by 16 Array Configuration

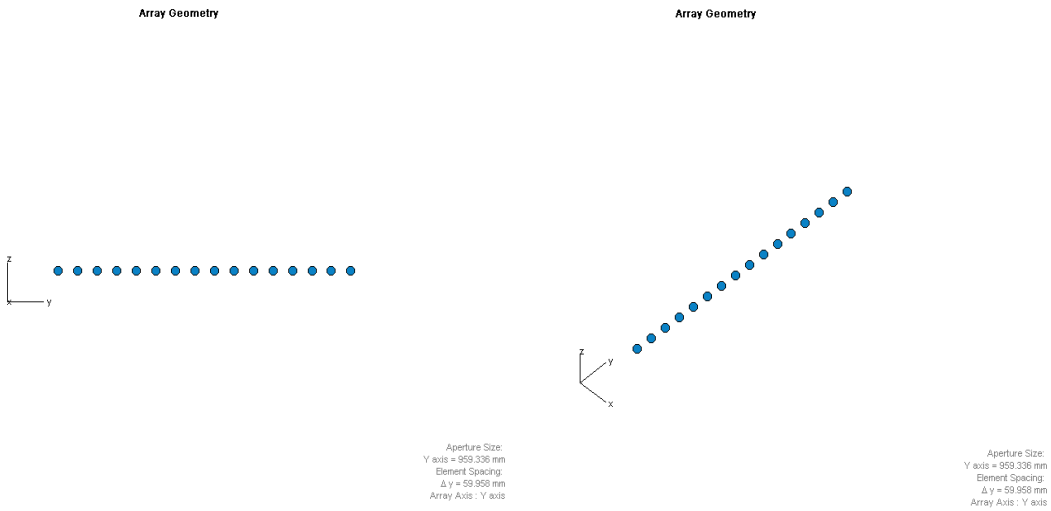

Fig. 16. The Linear Phased Array Configuration consisting of 16 antenna elements equally spaced $\lambda/2$.

2 by 8 Array Configuration

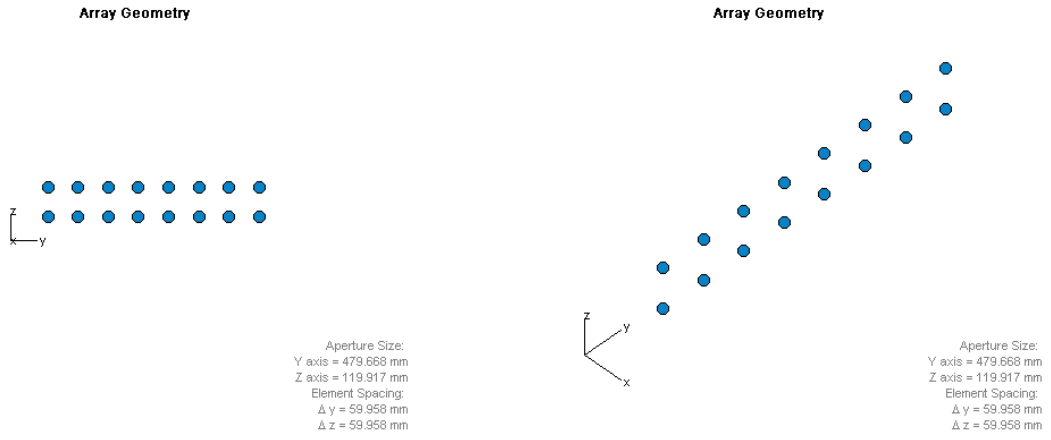

Fig. 17. The Planar Phased Array Configuration consisting of 8 by 2 antenna elements equally spaced $\lambda/2$ distance in both the horizontal and vertical direction.

4 by 4 Array Configuration

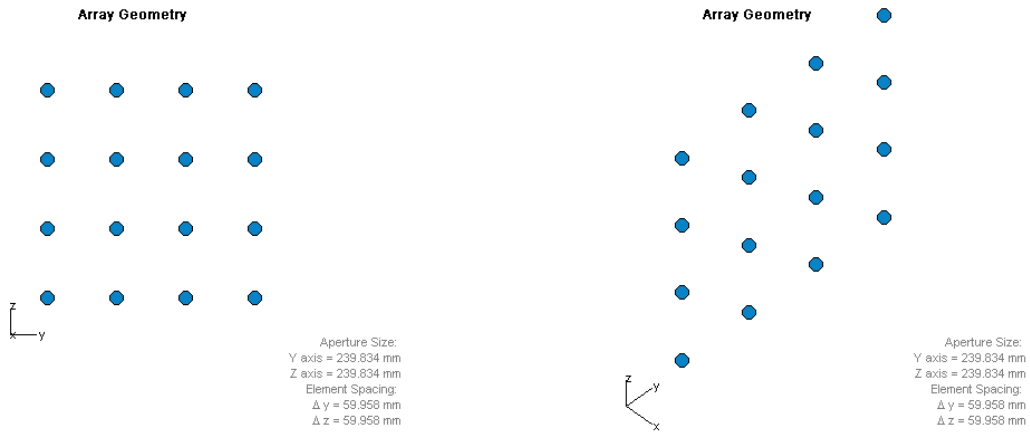

Fig. 18. The Planar Phased Array Configuration consisting of 4 by 4 antenna elements equally spaced $\lambda/2$ distance in both the horizontal and vertical direction.

Mapping Radiation Pattern on Area

With the antenna configurations described above, a radiation pattern from each can be obtained using the equations in Chapter II. However, in order to map the radiation pattern on the area, the signal strength and direction is projected onto the surface. Depending on the configuration and the direction the array is moved, a heat map of the radiation strength is created on the area. This heat map is analyzed in determining the quality of the uplink and downlink in transmission and reception.

Radiation Pattern

The radiation pattern of each phased array antenna configuration is constructed from Equation (22) in Chapter II.

$$E(\theta,\phi) = \sum_{m=1}^{M}\sum_{n=1}^{N} E_{ele}(\theta,\phi)e^{j*k*\sin(\theta)*(m*dx*\cos(\phi)+n*dy*\sin(\phi))} \quad (57)$$

So far, a significant portion of the variables in this equation have been defined. *M* and *N*, the horizontal and vertical element numbers, were defined such that $M * N$ total 16 elements. $E_{ele}(\theta,\phi)$, the element electric field, was defined to be 1, indicative of an omnidirectional element point source. *k*, the wave number, is equal to $\frac{2\pi}{\lambda}$. dx and dy, the element spacing, were defined to be $\frac{\lambda}{2}$. The wavelength λ is equal to $\frac{c}{f}$, where *c* is the speed of light and *f* is the transmitting frequency of 2.4 GHz.

It remains to define the azimuth and elevation angles, θ and ϕ respectively. More specifically, a resolution of these angles needs to be set in order to construct the radiation pattern. This resolution was determined to be 1 degree for both angles in order to keep the size of the resulting matrices (memory) and computation latency (delay) small. To elaborate, the azimuth and elevation angles are swept from -90 to 90 degrees in increments of 1 degree.

Projecting the Radiation Pattern on the Area

After the radiation pattern is calculated, it needs to be projected on the area to show the signal strength which can be received at the given locations (red squares in Fig. 13.) throughout the area. This process is similar to the projection of light on a surface in optics theory. Different light sources can have different projection patterns which favor certain scenarios, with all other parameters kept constant: power, source location,

direction of main beam, etc. An example of different projections in light sources is show in Fig. 19. below. This same principle applies to phased arrays.

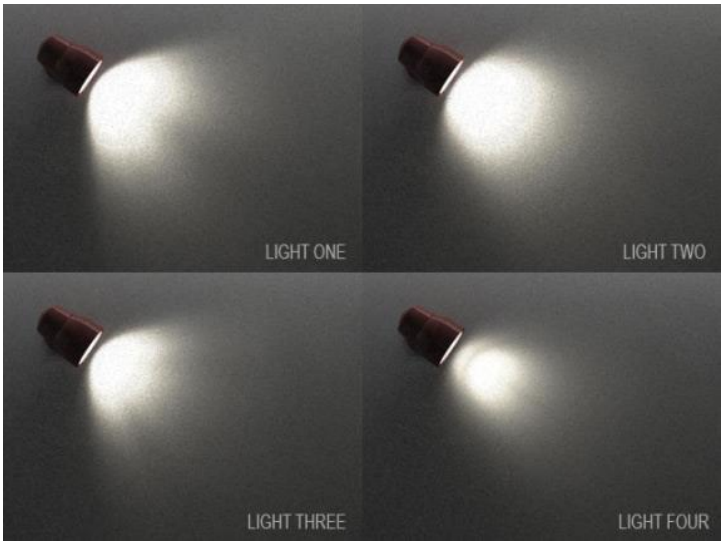

Fig. 19. The projection of light on a surface [18].

To calculate the projection of the radiation pattern, the first step is to decompose the radiation pattern vector of interest into its directional unit vector **u** and magnitude Q. The magnitude, Q, is equal to the radiation strength and the directional vector **u** which is composed of a unitary magnitude and an azimuthal angle and an elevation angle from Equation (22) in Chapter II. With the direction vector **u** established, the projection simplifies to an intersection of a line (**L**) and a plane (**P**). The vector **u** is extended until it meets the plane at which the receiver is positioned.

The line-plane intersection can be computed as follows. Given that the line **L** and plane **P** are not parallel, then **L** and **P** intersect in a unique point, $P(s_I)$ as displayed in Fig. 20.

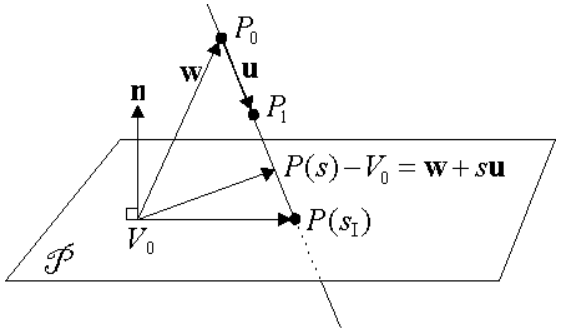

Fig. 20: Intersection of a line and a plane [2].

At the intersecting point, the vector

$$P(s) - V_0 = \boldsymbol{w} + s * \boldsymbol{u} \tag{58}$$

is perpendicular to **n**, the normal vector of the plane, and

$$\boldsymbol{w} = P_0 - V_0 \,. \tag{59}$$

This is equivalent to the dot product

$$\boldsymbol{n} \cdot (\boldsymbol{w} + s * \boldsymbol{u}) = 0 \,. \tag{60}$$

Solving for s_I the result is shown below [2]

$$s_I = \frac{-\mathbf{n} \cdot \mathbf{w}}{\mathbf{n} \cdot \mathbf{u}} = \frac{\mathbf{n} \cdot (\mathrm{V_0} - \mathrm{P_0})}{\mathbf{n} \cdot (\mathrm{P_1} - \mathrm{P_0})} \,. \tag{61}$$

After obtaining the location of this intersection, this coordinate is given a third dimension which corresponds to the radiation strength, or the magnitude of the original vector.

With the projection of the radiation pattern complete, some limitations can be observed. Because the resolution of the radiation pattern is 1 degree, the projection of the pattern sparsely intersects the intended area at large distances. A resolution of 1 degree, constructs a pattern with a total of 32761 points (*181 by 181*). Although this resolution may seem adequate, it is a shortfall for several reasons. First, because the antenna is stationary and cannot be readjusted as the direction of the beam changes, when the beam is analyzed toward higher elevation angles, the 1 degree resolution impedes the antenna radiation pattern from reaching certain locations within the area (example: red trajectory in Fig. 21.). Second, this limitation also occurs because the distance from the antenna to the intended receiving node is much greater than the height of the antenna. At these disproportional distances, less than 1 degree resolution in beam directivity is needed to reach the intended receivers. This inconsistency can be seen in Fig. 21.

To address these limitations an interpolation of the radiation strength is calculated based on a linear regression between adjacent radiation values

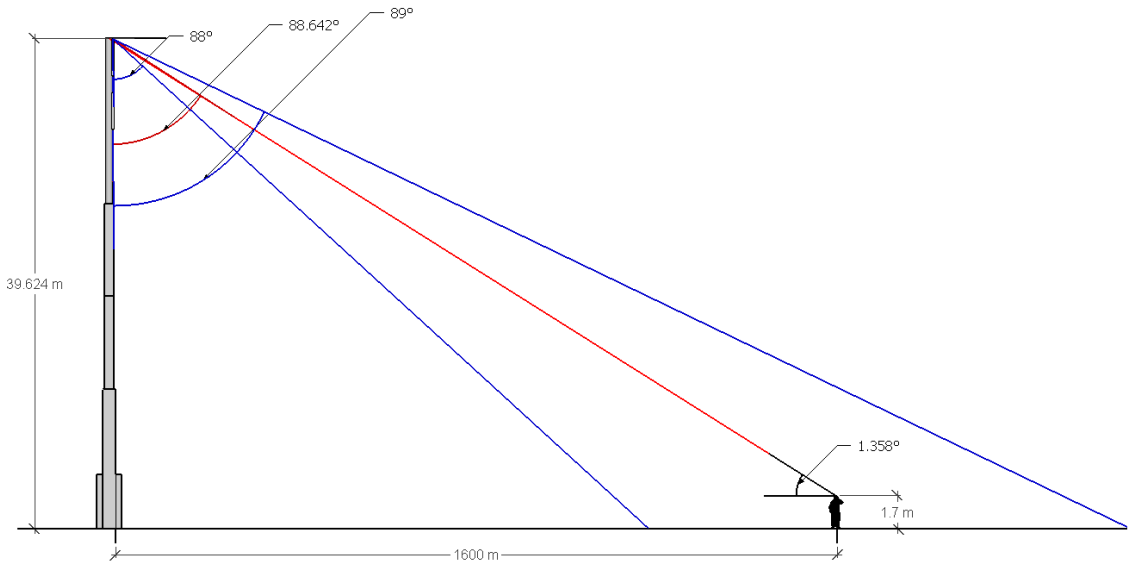

Fig. 21. Limitation in the 1 degree resolution of the radiation pattern. The blue trajectories of the radiation pattern represent vectors for which the pattern has a radiation stregth magnitude. However, the position where the receiver is located does not have a corresponding radiation strength, and the red trajectory does not exist in the radiation pattern. This is because the resolution of the radiation pattern is limited and because the distance to the user is much greater than the height of the antenna. *Not to scale.

Linear Interpolation

The principle of linear interpolation revolves around the concept of determining the value of an unknown coordinate point based on the values of two known points. If the two known points are given by the coordinates (x_0, y_0) and (x_1, y_1), the linear interpolation is the straight line between these points [19]. For a value *x* in the interval (x_0, x_1), its respective *y* value along the straight line is given by the equation:

$$\frac{y - y_0}{x - x_0} = \frac{y_1 - y_0}{x_1 - x_0} \tag{62}$$

which can be derived geometrically from Fig. 22.

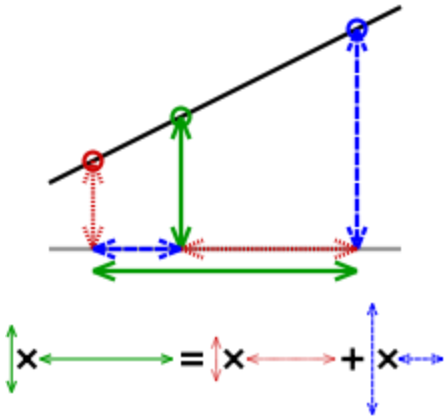

Fig. 22. Calculating the radiation strength based on linear interpolation [21].

In this geometric visualization, the value at the green circle multiplied by the distance between the red and blue circles is equal to the sum of the value at the red circle multiplied by the distance between the green and blue circles, and the value at the blue circle multiplied by the distance between the green and red circles.

Solving this equation for *y*, which is the unknown value at *x*, gives

$$y = y_0 + (y_1 - y_0)\left(\frac{x - x_0}{x_1 - x_0}\right) \tag{63}$$

the formula for linear interpolation in the interval (x_0, x_1) [19].

This formula can also be interpreted as a weighted average. The weights are inversely related to the distance from the end points to the unknown point; the closer point has more influence than the farther point. Thus, the weights are $\frac{x-x_0}{x_1-x_0}$ and $\frac{x_1-x}{x_1-x_0}$, which are normalized distances between the unknown point and each of the end points.

These linear interpolation properties are used in calculating the radiation strength on the surface of the area where the radiation pattern cannot be extended, due to the limitation in resolution of the elevation and azimuthal angles.

Transmission and Reception

Downlink

In determining the downlink efficiency, the line of sight direction from each receiver (red square in Fig. 13.) to the beacon antenna is determined. These direction vectors are then used to point the main antenna beam towards every receiver one after the other. After the beam is directed toward the intended receiver, the radiation strength from the antenna to that receiver is recorded. With the radiation strengths computed for all receivers, the decay factor from Chapter II is applied and the expectation a variance of these signal strengths are calculated with the equations from Chapter II.

Uplink

On the reverse, to quantify the efficiency of the uplink, the interference is the main parameter analyzed. Two scenarios are emphasized. The first is determining the expectation of the interference, and the second is determining the variance of the interference. In the first scenario, the location of the receiver is first chosen. This is the intended user which communicates with the beacon. At every other location in the area, an interferer can be present with equal likelihood. This interferer can disturb the uplink quality between the beacon and the receiver. After the mapping of the radiation pattern

on the area is done, the signal strength at the intended receiver location is determined and subtracted from the sum of all the other received points. This quantity represents the total interference given the location of the intended receiver. This total interference is re-calculated for every receiver location in the area. The expectation of all these results is computed to obtain the final result, the expectation of the interference. The equations to use in obtaining these results are given in Chapter II.

In the second scenario the computation of the variance is calculated utilizing the same receiver and interferer setup as in the downlink. The equations in Chapter II are used step by step, to calculate the variance of the interference. To compare the efficiency of all antenna configurations, the above calculation procedures are made and analyzed for every antenna configuration.

CHAPTER IV

SIMULATED RESULTS

Chapter IV focuses on the obtained simulated results from the system model described in Chapter III and the theoretical background established in Chapter II. The conclusions drawn from these results are covered in Chapter V.

Area Revisited

As was mentioned in Chapter III, the area is divided by a 50 by 50 grid with red squares marking desired receiver locations. There are 1200 total receiver points. However, in Fig. 23. this area was changed to a 50 by 51 grid to show how the patterns compare.

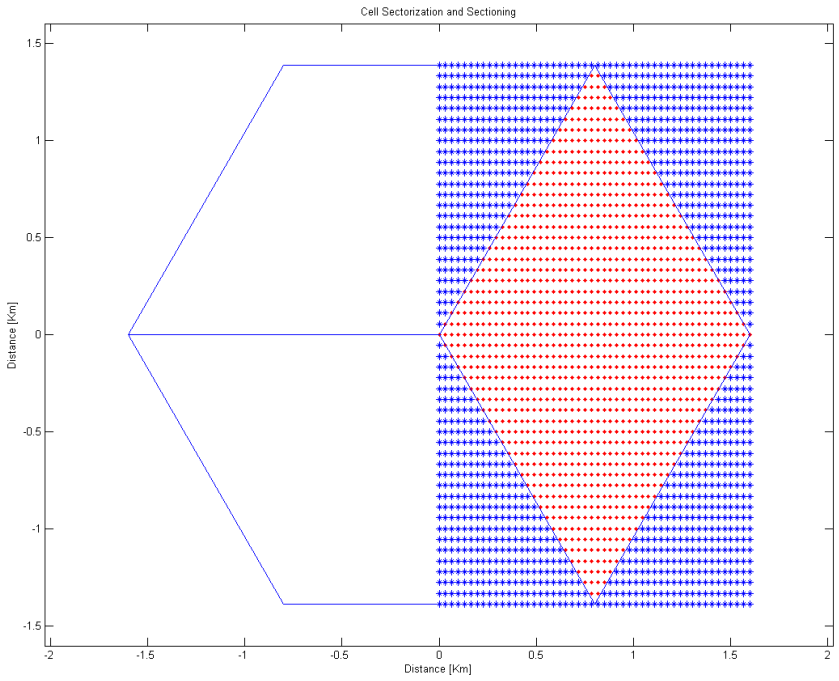

Fig. 23. Desired area and placement of receivers.

Radiation Patterns

To simulate the radiation pattern for each antenna configuration (1 by 16, 2 by 8, and 4 by 4), Equation (22) from Chapter II is used:

$$E(\theta,\phi) = \sum_{m=1}^{M}\sum_{n=1}^{N} E_{ele}(\theta,\phi)e^{j*k*\sin(\theta)*(m*dx*\cos(\phi)+n*dy*\sin(\phi))}.$$

In creating this radiation pattern, isotropic radiation elements are used and the variables in the equation above are replaced according to each array pattern; the azimuth and elevation angles are swept from -90 to 90 degrees in increments of 1 degree as discussed in Chapter III. The radiation pattern of an isotropic element is simulated in Fig. 24.

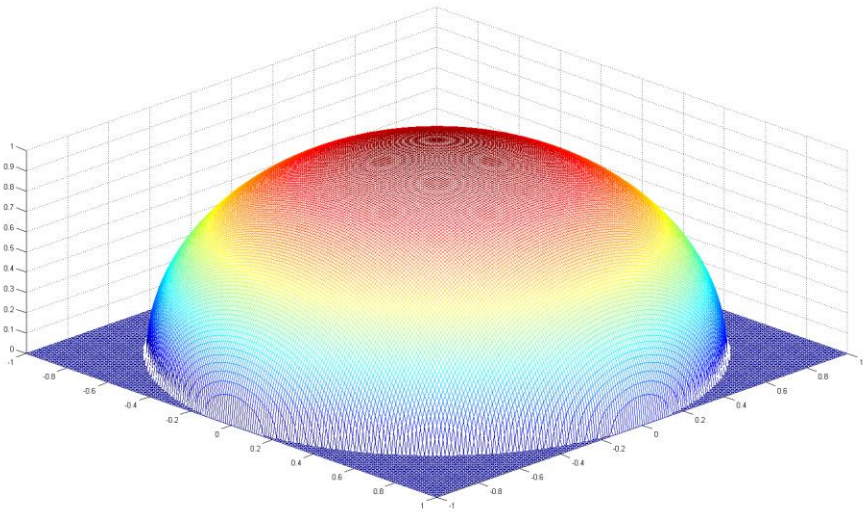

Fig. 24. Isotropic radiation element.

Following the antenna models in Fig. 25., all parameters are kept constant for the three arrays other than antenna configurations. An example in which the beam is directed toward $\theta = 0°, \phi = 0°$ for all patterns is shown in Fig. 25.

Projecting Radiation Pattern to Area

Once the radiation pattern for each antenna is simulated, the next step is obtaining the projection of these patterns on the intended surface. To accomplish, this Equation (61) from Chapter III is used. The results from projecting the patterns in Fig. 25., for which the beam is directed toward $\theta = 0°, \phi = 0°$ for all patterns, are shown in Fig. 26. In obtaining this figure, linear interpolation was also applied as discussed in Chapter III.

From Area to Grid (Linear Interpolation)

Although the radiation pattern is mapped to the area, the location of the radiation points at which the projection was created may not directly match the position of the intended receiver points (red marks in Fig. 23). To acquire radiation values for the intended receiver points, the linear interpolation technique from Chapter III is applied to the projection map. The results are shown in Fig. 27. for the antenna patterns in Fig. 25.

Applying the Free Space Path Loss

With the signal strengths established for intended receivers on the area, the free space path loss theory from Chapter II is applied to the interpolated data. After applying this path loss, the results are further used to quantify the downlink and uplink efficiency.

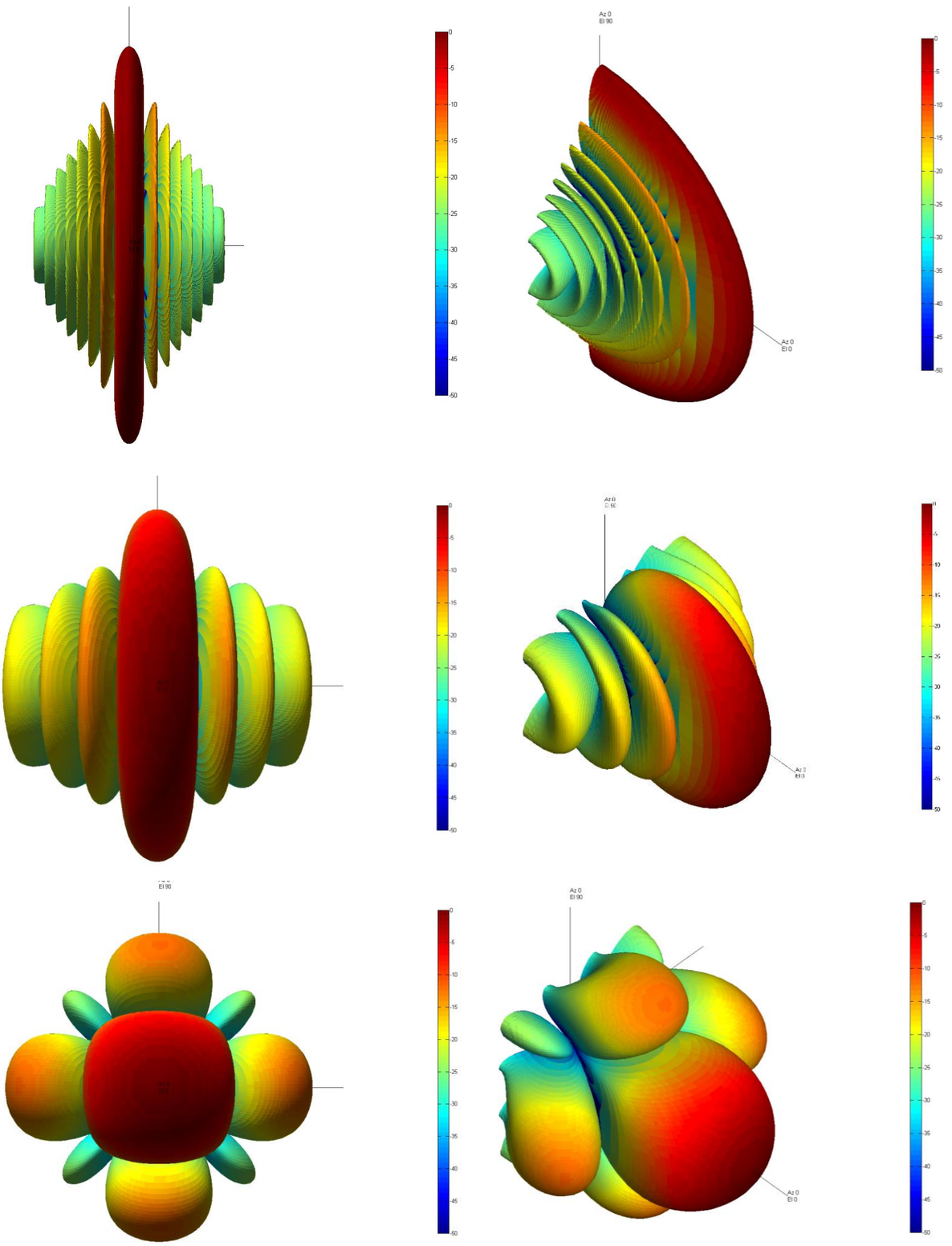

Fig. 25. Radiation patterns of 1 by 16 (Top) 2 by 8 (Middle) and 4 by 4 (Bottom). On the left side these patterns are viewed from the front and on the right side they are viewed from a 45° elevation 45° azimuth reference. The radiation patterns of all configurations are normalized and the main beam is directed to have an azimuthal angle of 0° and an elevation angle of 0°.

Downlink

The procedure for quantifying the downlink efficiency was introduced in Chapter II. To summarize this process, the optimal received signal strength is first obtained. The optimal power is the highest received signal strength from the antenna to each receiver location. This occurs when the main beam is directed towards the receiver and the antenna forms a straight line of sight with the receiver. The optimal power is computed for every receiver point (red square in Fig. 23.) and shown in Fig. 28. after which the free space path loss is applied to the power at every receiver; Fig. 29. shows how path loss impacts the pattern of a beam directed along the x-axis. For observational purposes, this procedure was repeated with the area sectioned by a 50 by 51 grid. The results are shown in Fig. 30. and Fig. 31. Lastly, the statistical expectation is then calculated with equations in Chapter II and the following results were obtained.

Table 1
Downlink Expectation

	Antenna Configuration		
	1X16	2X8	4X4
$E[X]$	1.2855*H	1.2890*H	1.2896 *H

*Where H = 1/(Area of sector).

Uplink

The procedure for quantifying the uplink efficiency is introduced in Chapter II and is revisited in this section. In this procedure, an emphasis was placed on calculating the

expectation and variance of the interference. The expectation of the interference given the location of the receiver is modeled as follows:

$$E[X|location\ of\ x_i] = [(x_1 + x_2 + \cdots + x_k) - x_i] * c \quad (64).$$

By summing all the interferences at every location, the average interference across the sector can be obtained. These results are recorded in Table 2 for all of the antenna patterns. The results for the simulation of the expectation of the interference can be seen in Fig. 32.

The variance of the interference is modeled by the law of total variance

$$Var(X) = \underbrace{E[Var(X|Y)]}_{1} + \underbrace{Var(E[X|Y])}_{2} \quad (65)$$

which is broken down as:

1) The expected value of the conditional variance: $E[Var(X|Y)]$
2) The variance of the conditional means: $Var(E[X|Y])$.

To compute the total variance, the focus is placed on the first part of the equation, the expected value of the conditional variance. First $Var(X|Y)$ is computed and displayed in Fig. 33. Next, the expectation was calculated and is recorded in Table 3. In the second part of the equation, the variance of the conditional means is rewritten as:

$$Var(E[X|Y]) = E\left(\left[E(X|Y) - E\big(E(X|Y)\big)\right]^2\right) = E([E(X|Y) - E(X)]^2). \quad (66)$$

The quantity $[E(X|Y) - E(X)]^2$ is computed, after which the expectation is calculated and the value for $Var(E[X|Y])$ is recorded in Table 3. The total variance is obtained by adding the quantities above. The results are recorded in Table 3.

Table 2
Computing the Uplink Interference Expectation

	Antenna Configuration		
	1X16	2X8	4X4
$E[X]$	0.0341*H	0.0765*H	0.1445*H

*Where H = 1/(Area of sector).

Table 3
Computing the Uplink Interference Variance

	Antenna Configuration		
	1X16	2X8	4X4
$E[Var(X\|Y)]$	2.6209e-04*H	2.3610e-04*H	1.9502e-04*H
$Var(E[X\|Y])$	0.1139*H	0.0778*H	0.2149*H
$Var(X)$	0.1142*H	0.0780*H	0.2151*H

*Where H = 1/(Area of sector).

quantity $[E(X|Y) - E(X)]^2$ is computed, after which the expectation is calculated and the value for $Var(E[X|Y])$ is recorded in Table 3. The total variance is obtained by adding the quantities above. The results are recorded in Table 3.

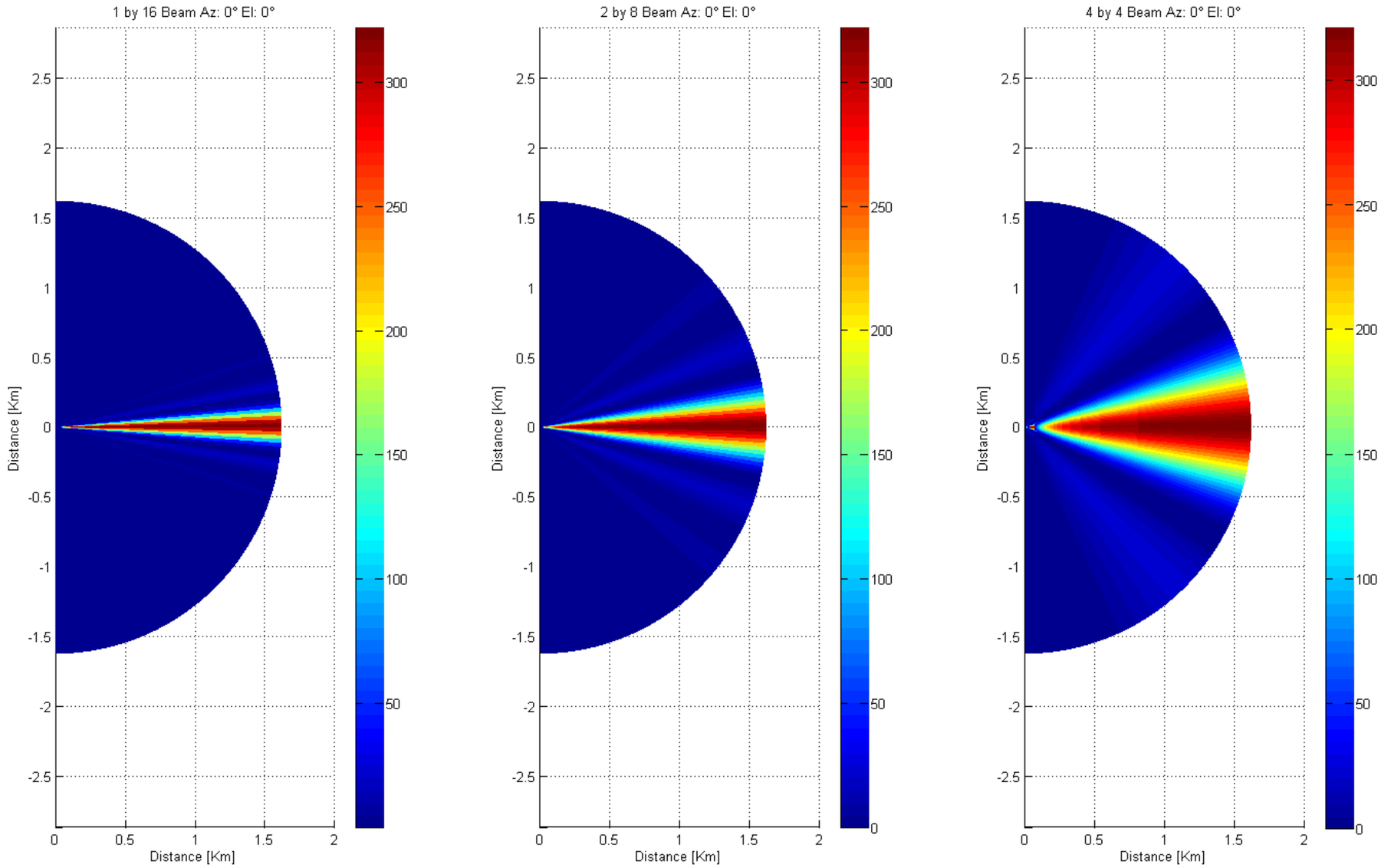

Fig. 26. The power of each antenna pattern is projected on the respective area and linear interpolation is applied.

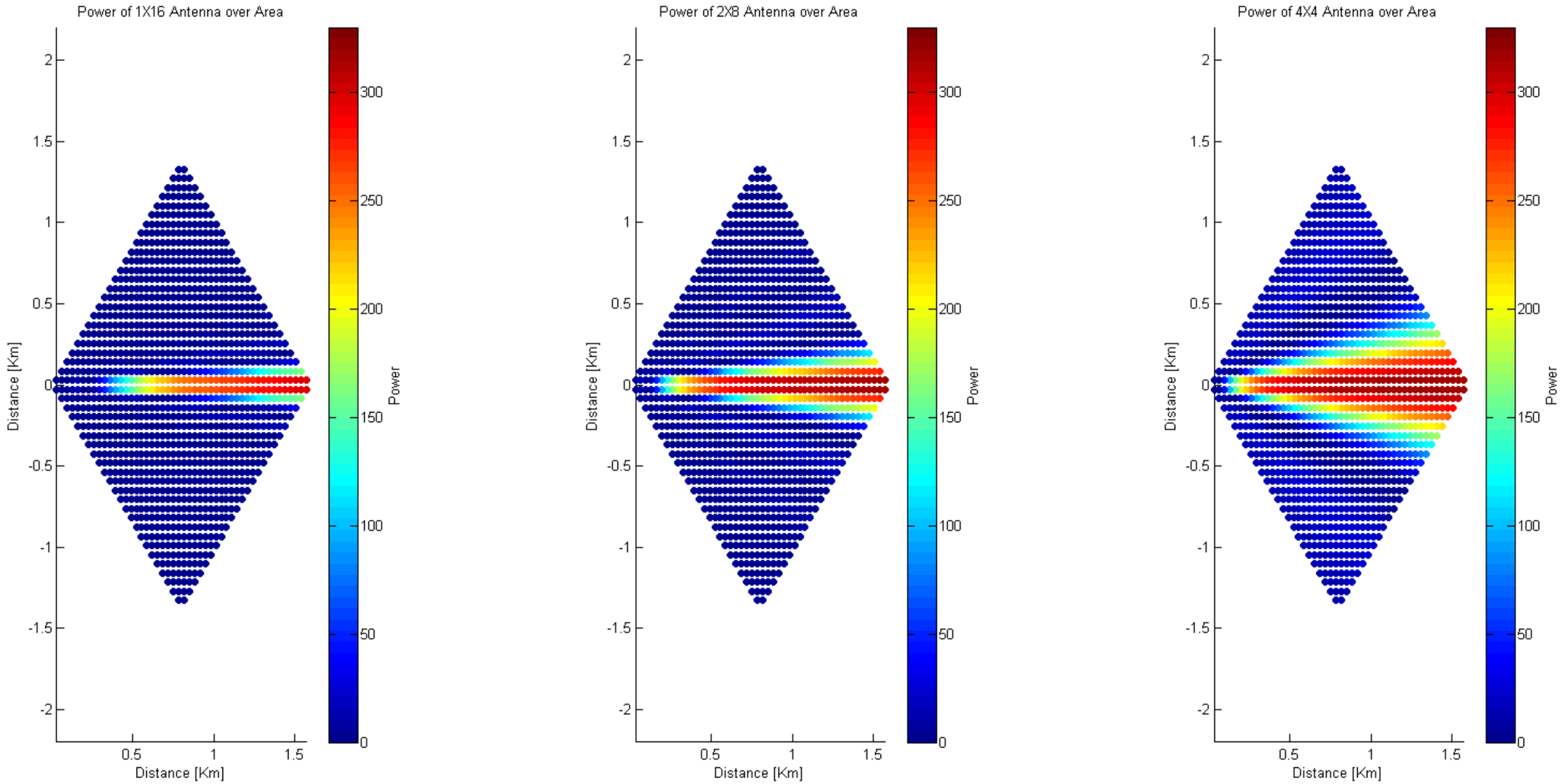

Fig. 27. As projecting the radiation pattern to every receiver, the power of each antenna pattern at every point is obtained. The antenna is steered in the 0° elevation, 0° azimuth direction, or more concisely along the positive x-axis. The power is scaled, from 0 to 330, equally for all patterns. There are 1200 total points within the area.

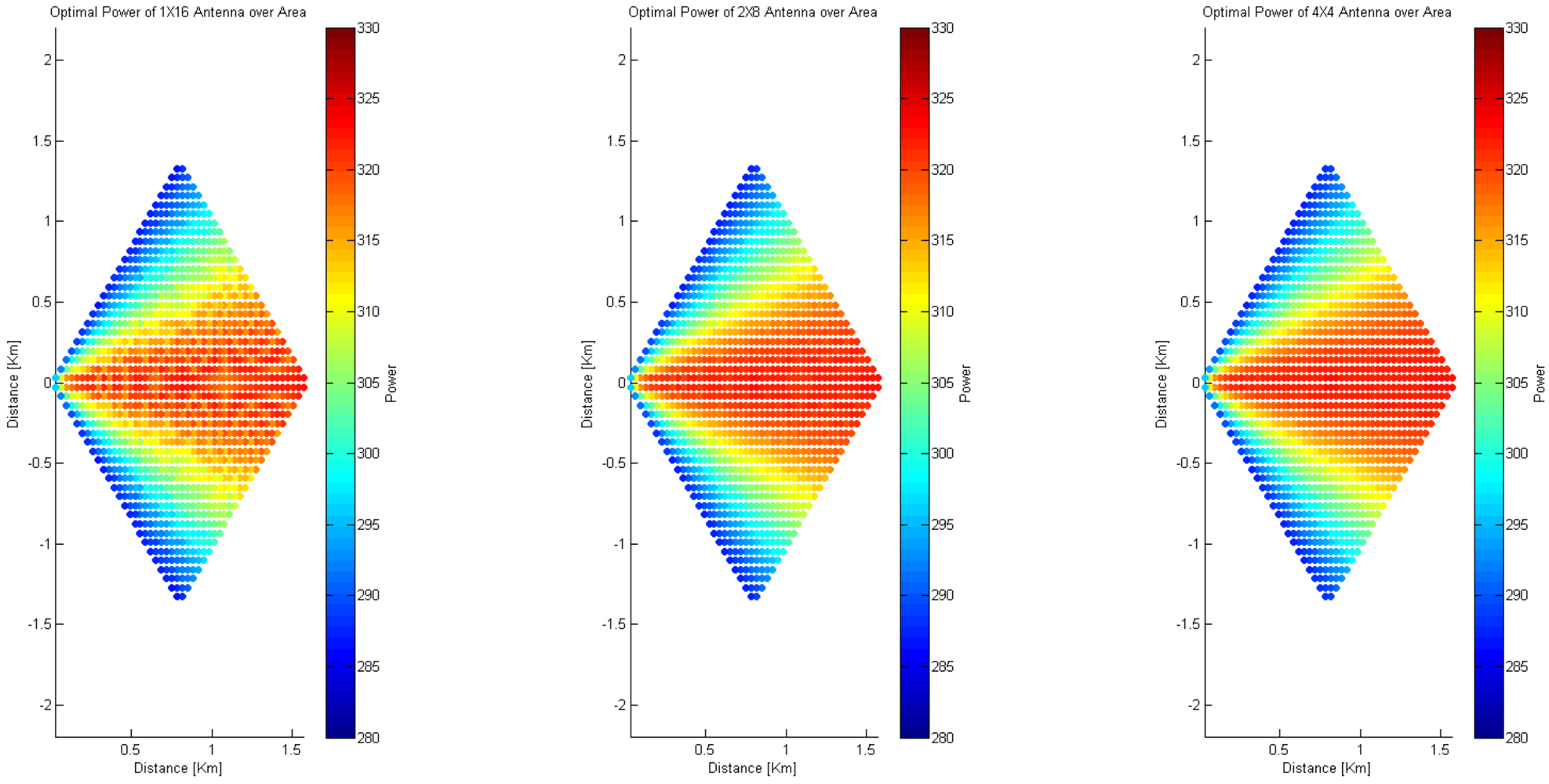

Fig. 28. The optimal received radiation strength with no path loss at every grid point. The optimal power is obtained by steering the beam of the antenna to each grid point and recording the maximum power at that point. The power is scaled, from 280 to 330, equally for all patterns. There are 1200 total points within the area.

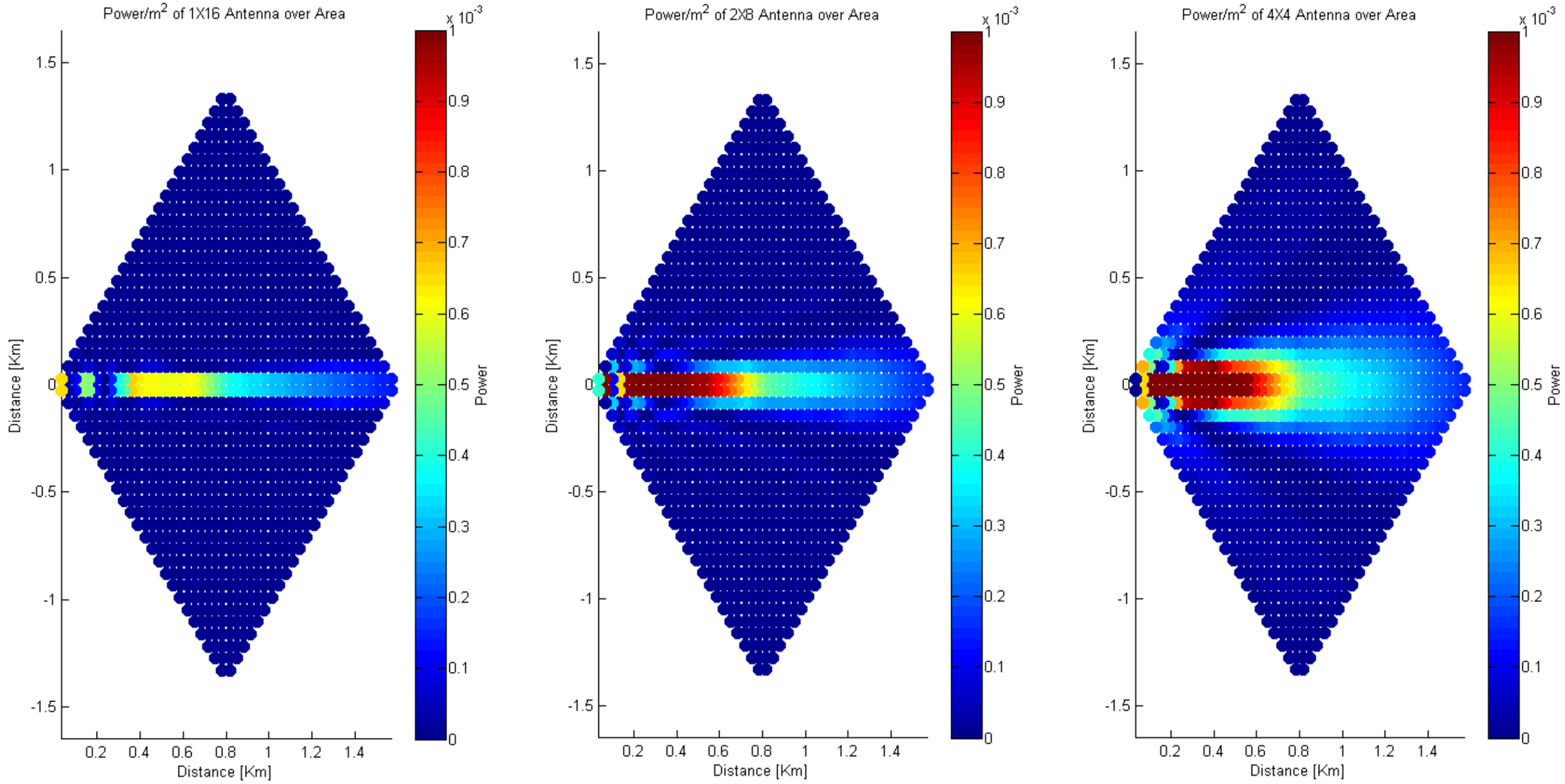

Fig. 29: Power as a function of distance or power decay (Intensity) of each antenna pattern at every grid point. The antennas are steered in the 0° elevation, 0° azimuth direction, or more concisely along the positive x-axis. The intensity is scaled, from 0 to 0.001, equally for all patterns. There are 1200 total points within the area.

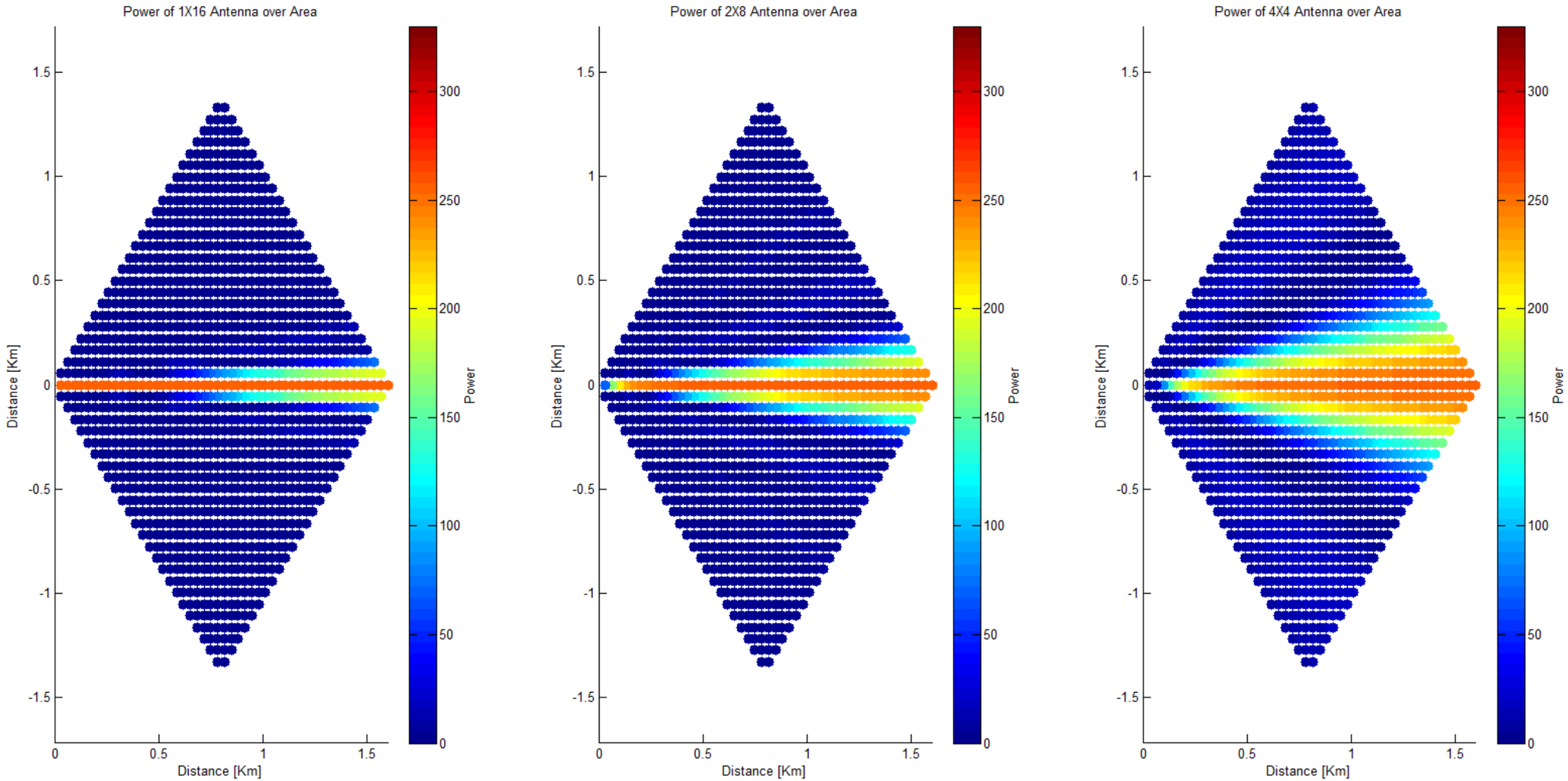

Fig. 30. Projecting the radiation pattern to the area divided by a 50 x 51 grid and applying linear interpolation. The power of each antenna pattern is computed at every grid point (50x51). The antenna is steered in the 0° elevation, 0° azimuth direction, or more concisely along the positive x-axis. The power is scaled, from 0 to 330, equally for all patterns. There are 1250 total points within the area.

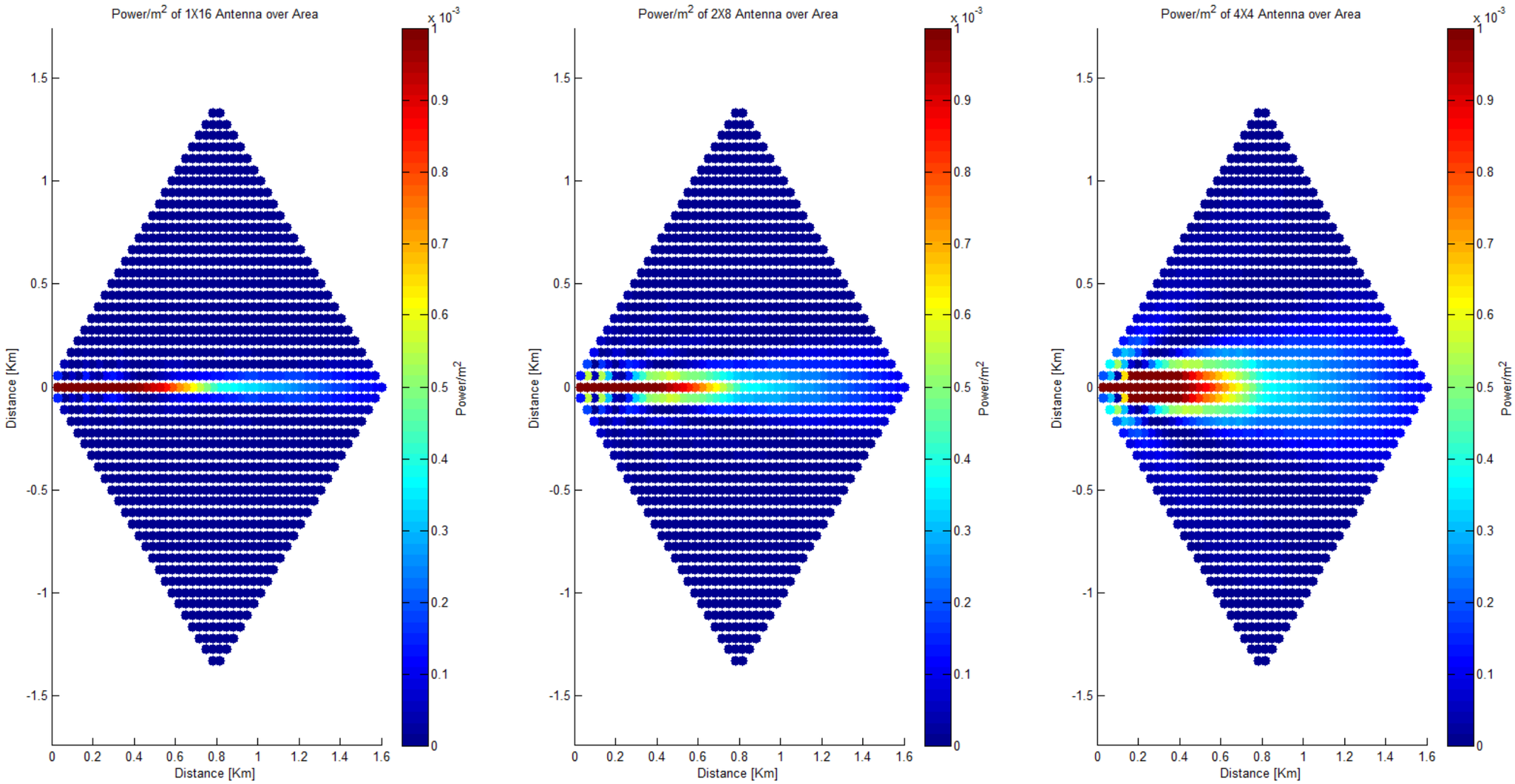

Fig. 31. Power as a function of distance or power decay (intensity) of each antenna pattern at every grid point on a 50 x 51 grid. The antennas are steered in the 0° elevation, 0° azimuth direction, or more concisely along the positive x-axis. The intensity is scaled, from 0 to 0.001, equally for all patterns. There are 1250 total points within the area.

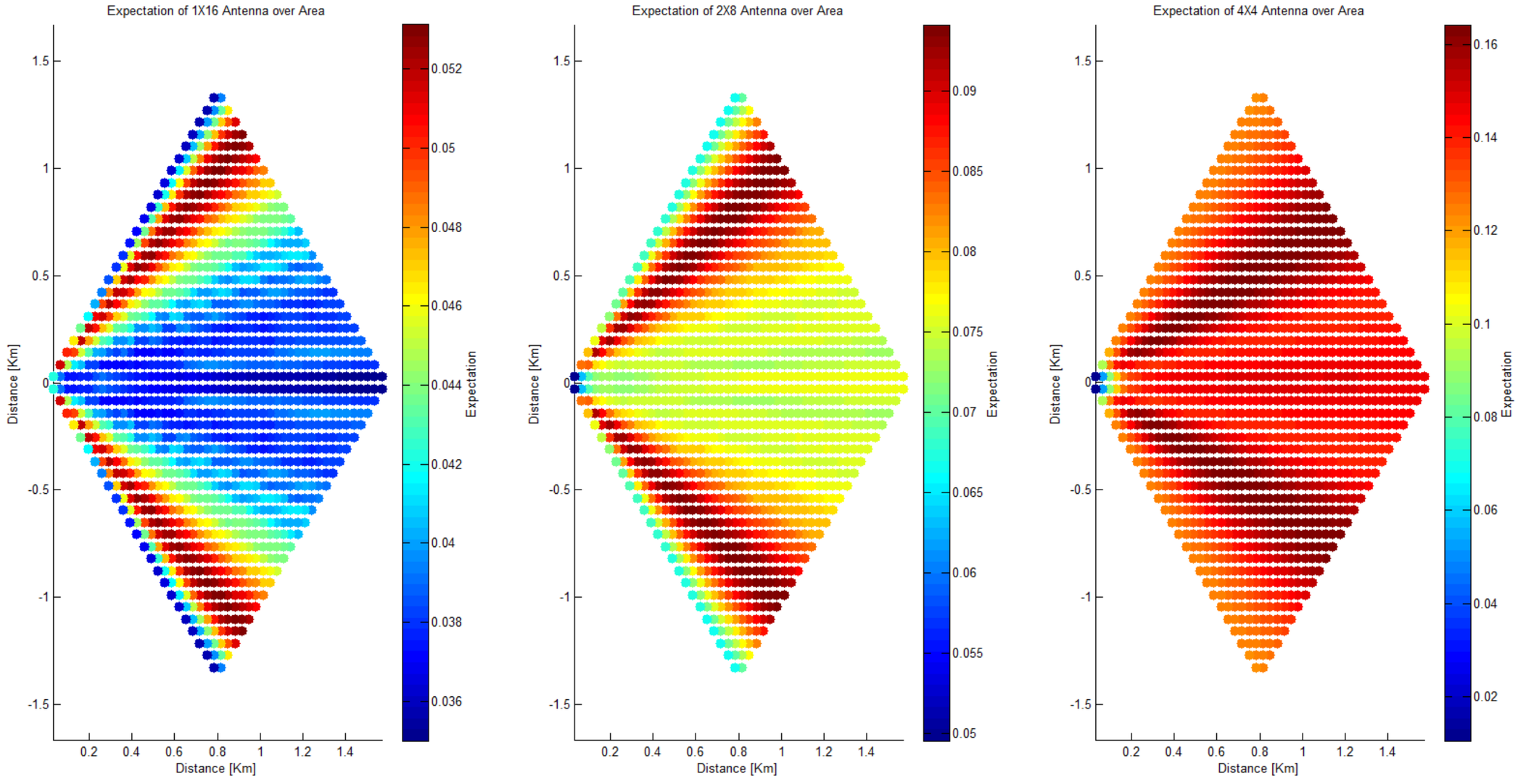

Fig. 32. Uplink Interference Expectation: the expectation of the interference, with distance decay, for each antenna pattern at every grid point (50x50). The expectation was calculated with power taken in units of Watts. The scale of each graph is different based on maximum and minimum expectation values of each. There are 1200 total points within each area.

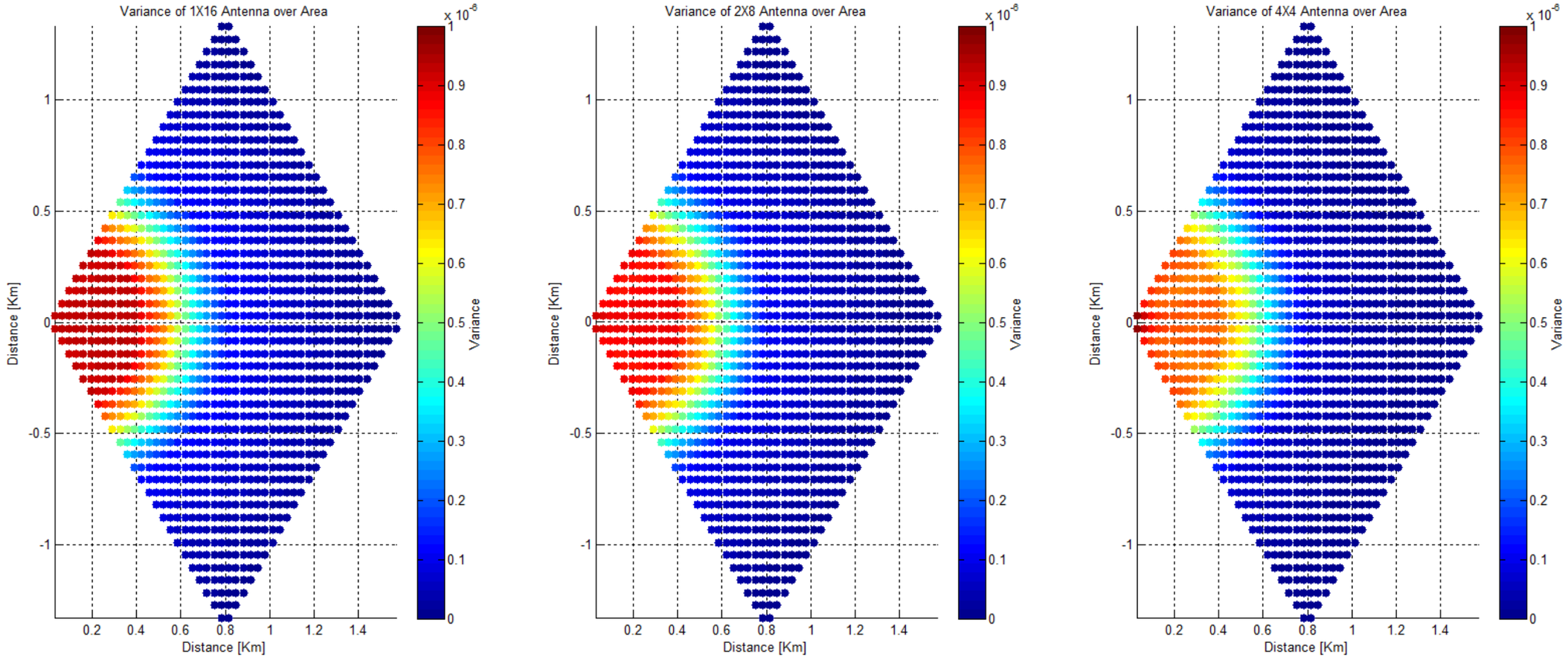

Fig. 33. Variance of the power, with distance decay, for each antenna pattern at every grid point (50x50). The variance was calculated with power taken in units of Watts. The scale of each graph is different based on their maximum and minimum expectation values. There are 1200 total points.

CHAPTER V

CONCLUSIONS

The results obtained in Chapter IV emphasize significant information about the capabilities of each antenna configuration to establish successful communication on the uplink and downlink. Looking at the downlink results, it can be observed that the 4 by 4 PAA configuration is best at directing the beam throughout the sector to each receiver. The 8 by 2 PAA comes in second by a slight margin and the 1 by 16 linear PAA comes in last. After observing the uplink results, a complete picture of the configuration capabilities is shown. The 4 by 4 PAA configuration experienced the largest average amount of interference. The 2 by 8 and 1 by 16 followed respectively. However, the variance of the interference shows that the 4 by 4 PAA's interference varies the most. The 1 by 16 and 2 by 8 PAAs show less variance of interference.

With these results, several conclusions about the performance of each antenna can be drawn. For example, if the transfer of information is of uttermost importance, and no regard is given toward signal integrity, interference, or jamming, the 4 by 4 PAA configuration would be the best candidate. This scenario can be a setting which consists of only one receiver in an environment having no interference. If interference is rampant and a high priority is given toward signal integrity, the 1 by 16 or 2 by 8 PAA configuration would be the best performers. Although a lower downlink performance is obtained by the 2 by 8 in comparison to the 4 by 4, the ability of this antenna to avoid

interference is much better than that of the 4 by 4. Lastly, the 1 by 16 shows the lowest average interference; however, in comparison to the 2 by 8, the 1 by 16 PAA has a larger variance in the spread of this interference because it is not able to redirect its beam vertically. To outweigh one configuration over the other, the locations and movement patterns of the receiver need to be further analyzed. If the receiver sporadically moves on the periphery of the sector, the 2 by 8 may perform best; however, if the receiver predictively moves only within the center of the sector the 1 by 16 may outweigh the 2 by 8 pattern's transmitting performance.

Several continuations of this study can be conducted to experimentally determine the accuracy of the simulated results. Furthermore, in the construction of the PAA configurations different variables can be taken into account to also show how they compare with the baselines in this study. Diverse PAA properties such as: antenna elements, element spacing, and element number, can be used to show and compare performance analytics. In addition, the size and shape of the geographical area of study can be changed to mirror more dense environments. Taking an even greater step, the mobility of the antenna is a further variable which can be introduced. In this study the antenna was assumed to be stationary, and facing the 0 degree azimuth and 0 degree elevation direction. However, with a capability of moving the elevation angle certain configurations with low resolutions on the vertical axis (such as the 1 by 16) could benefit tremendously. Experiments analyzing these "hybrid" antennas can be conducted to show if the mechanical leverage could add more accuracy in performance and

communication while at the same time endure stress tests or keep up with the movements of receivers. A great limitation encountered in this study was the resolution of the shift angle of the antenna radiation pattern. In further studies, this resolution can be diminished to obtain a more accurate patterns. With the advent of more technological improvements, these small resolutions may be achievable by hardware.

REFERENCES

[1] D. Ehyaie, 'Novel Approaches to the Design of Phased Array Antennas', Doctor of Philosophy, The University of Michigan, 2011.

[2] D. Sunday, 'Intersections of Lines, Segments and Planes (2D & 3D)', *Geomalgorithms.com*, 2015. [Online]. Available: http://geomalgorithms.com/a05-_intersect-1.html. [Accessed: 18- Feb- 2015].

[3] S. P. Stapleton, G. S. Quon, , 'A cellular base station phased array antenna system,' *Vehicular Technology Conference, 1993., 43rd IEEE* , vol., no., pp.93,96, 18-20 May 1993.

[4] P. Bevelacqua, 'Antenna Arrays', *Antenna-theory.com*, 2015. [Online]. Available: http://www.antenna-theory.com/arrays/main.php. [Accessed: 18- Feb- 2015].

[5] A. Rivas, 'Implementation of Phased Array Antenna Technology Providing a Wireless Local Area Network to Enhance Port Security and Maritime Interdiction Operations', Masters, Naval Postgraduate School, 2009.

[6] H. Visser, *Array and phased array antenna basics*. Chichester: Wiley, 2005.

[7] K. F. Braun, 'Electrical Oscillations and Wireless Telegraphy.' Nobel Lecture, December 11, 1909. *Nobel Lectures in Physics 1901-1921* (Singapore: World Scientific Publishing Co.).

[8] S. Mondal, A. Sinha and J. Routh, '5 International Journal of Advance Research in Science and Engineering- IJARSE, Vol-1, Iss-2 A Survey on Evolution of Wireless Generations 0G to 7G',*International Journal of Advance Research in Science and Engineering*, vol., no. 2, p. 3, 2015.

[9] R. Graf, *Modern dictionary of electronics*. Boston: Newnes, 1999.

[10] J. Hilbertsson and J. Magnusson, 'Simulation and Evaluation of an Active Electrically Scanned Array (AESA) in Simulink', Masters, Chalmers University of Technology, 2009.

[11] M. Lanne, 'Antenna array systems: electromagnetic and signal processing aspects', Masters, Chalmers University of Technology,2005.

[12] R. Hansen, *Phased array antennas*. Hoboken, N.J.: Wiley, 2009.

[13] IEEE Standard Definitions of Terms for Antennas. [Accessed: 18- Feb- 2015].

[14] A. Goldsmith, *Wireless communications*. Cambridge: Cambridge University Press, 2005.

[15] NTIA Seeks Input on Broadband Stimulus Money undated. [Online]. Available: http://www.accel-networks.com/blog/2009/03/ntia-seeks-input-on-broadband-stimulus.html. [Accessed: 18- Feb- 2015].

[16] Steelintheair.com, 'Cell Tower Heights Across the US', 2007. [Online]. Available: http://www.steelintheair.com/Blog/2007/09/cell-tower-heights-across-the-us.html. [Accessed: 18- Feb- 2015].

[17] C.D. Fryar, Q. Gu, C.L. Ogden, 'Anthropometric reference data for children and adults: United States, 2007–2010'. National Center for Health Statistics. Vital Health Stat 11(252). 2012.

[18] Cgarena.com, 2015. [Online]. Available: http://www.cgarena.com/freestuff/tutorials/max/ieslights/lights.jpga. [Accessed: 18- Feb- 2015].

[19] M. Hazewinkel, 'Linear interpolation', *Encyclopedia of Mathematics*: Springer, 2001.

[20] Wikipedia, 'List of WLAN channels', 2015. [Online]. Available http://en.wikipedia.org/wiki/List_of_WLAN_channels. [Accessed: 18- Feb- 2015].

[21] Wikipedia, 'Linear Interpolation Visualisation', 2015. [Online]. Available https://upload.wikimedia.org/wikipedia/commons/a/aa/Linear_interpolation_visualisation.svg. [Accessed: 18- Feb- 2015].

[22] J. Jensen, 'A Cognitive Phased Array Using Smart Phone Control,' Masters, Texas A&M University, 2012.